American Journal of Scholarly Research and Innovation

Volume: *16;* ***Issue:*** *5*
Pages: *01–26*
eISSN: 3067-2163

Digital Twin–Based Corrosion-Fatigue Crack Growth Prediction in 316L Stainless Steel and Alloy 690 for Nuclear Primary-Circuit Integrity Assessment

Efat Ara Haque[1];

[1]. Calibration Engineer, Baker Hughes Project, Pasadena, Texas, USA;
M.S. in Mechanical Engineering, Lamar University, Beaumont, Texas, USA, 2024
B.S. in Mechanical Engineering, Rajshahi University of Engineering and Technology (RUET), Bangladesh; Email: efatarahaque@gmail.com

Doi: 10.63125/6jpjqp76
Received: *23 February 2026;* ***Revised:*** *04 March 2026;* ***Accepted:*** *11 April 2025;* ***Published:*** *02 May 2026;*

Abstract

This study develops a digital-twin framework for corrosion-fatigue crack-growth prediction and integrity assessment of Type 316L austenitic stainless steel and nickel-base Alloy 690 in pressurized-water-reactor primary-circuit environments. The proposed framework couples linear-elastic fracture mechanics, a Paris–Walker-type crack-growth core, material- and environment-dependent acceleration terms, sequential Bayesian updating, uncertainty quantification, and risk-informed inspection logic. The research is structured as a physics-informed simulation study supported by verified literature and nuclear-industry standards rather than as a report of new plant or laboratory measurements. A synthetic population of 800 crack-growth trajectories is used to stress-test model behavior across material class, loading frequency, stress ratio, temperature, dissolved-hydrogen surrogate, cold-work state, initial flaw size, and critical crack size. Three prognostic strategies are compared: a static Paris-law baseline, an environment-corrected static model, and the proposed continuously updated digital twin. In the synthetic evaluation, sequential updating materially reduces remaining-useful-life error, improves crack-size tracking, and produces substantially better calibrated uncertainty intervals than static approaches, particularly under heterogeneous material and environmental states. The study also demonstrates how the twin can translate posterior crack-growth states into probability-of-threshold-exceedance estimates and inspection recommendations without replacing code-required flaw evaluation or engineering authorization. The principal contribution is an integrated integrity-assessment architecture that connects experimentally established corrosion-fatigue and primary-water stress-corrosion-cracking mechanisms with state-synchronized digital-twin prognostics for safety-critical nuclear primary-circuit components. The framework is intended as a research methodology that can later be calibrated and validated using qualified fatigue-crack-growth, environmentally assisted cracking, nondestructive examination, plant transient, and water-chemistry datasets.

KEYWORDS
Digital Twin; Corrosion Fatigue; Fatigue Crack Growth; 316L Stainless Steel; Alloy 690;

INTRODUCTION

Primary-circuit integrity in pressurized water reactors depends on the continued ability of pressure-boundary and internal components to tolerate cyclic mechanical and thermal loads while exposed to high-temperature aqueous environments. Austenitic stainless steels and high-chromium nickel-base alloys are central to this problem because they combine favorable mechanical properties with corrosion resistance, yet neither class is completely decoupled from environmentally assisted degradation. The U.S. Nuclear Regulatory Commission has long recognized that light-water-reactor coolant environments can reduce fatigue resistance relative to air and has incorporated environmental fatigue concepts through NUREG/CR-6909 and Regulatory Guide 1.207 (Chopra & Stevens, 2018; NRC, 2018). ASME Section XI, in parallel, provides the inservice inspection, flaw evaluation, acceptance, and repair/replacement framework by which degradation is managed in operating light-water-cooled nuclear plants (ASME, 2025).

Type 316 and 316L stainless steels are widely used in nuclear systems and have been studied extensively for environmentally assisted fatigue and stress-corrosion behavior in simulated PWR primary water. Experimental work has shown that the PWR environment can accelerate fatigue crack propagation and thereby reduce fatigue life, with sensitivity to loading rate, strain range, water chemistry, material condition, and crack-tip processes (Kamaya, 2013; Kamaya, 2017; Kamaya, 2020). Detailed crack-growth and microstructural investigations have further identified the influence of slip localization, hydrogen-related processes, sulfur level, cold or warm work, dissolved hydrogen, oxide stability, and crack-path crystallography (Mukahiwa et al., 2018; Choi et al., 2016). These observations show why a single stationary crack-growth coefficient is often insufficient for long-duration integrity prognosis.

Alloy 690 was introduced as a higher-chromium alternative to Alloy 600 for applications requiring improved resistance to primary-water stress corrosion cracking. Its service record and laboratory evidence demonstrate substantially improved resistance, but laboratory studies also show that Alloy 690 is not mathematically equivalent to a non-degrading material. PWSCC growth can be promoted by heavy cold work, unfavorable metallurgical condition, grain-boundary carbide morphology, local strain, oxidation processes, and other microstructural factors (Yonezawa et al., 2015; Zhai et al., 2017; Kuang et al., 2018). High-resolution studies have linked crack initiation to grain-boundary oxidation and diffusion-induced grain-boundary migration under dynamic straining, while NRC-sponsored programs have investigated crack-growth susceptibility and the effects of cold work in Alloy 690 and related weld metals (Bruemmer et al., 2012; Toloczko et al., 2016; Kuang & Was, 2020).

The integrity-management challenge is therefore not simply to identify a single "best" crack-growth curve. Instead, the assessment must represent the evolving state of a particular component, including its current flaw size, load history, thermal history, water-chemistry exposure, material condition, inspection uncertainty, and the uncertainty of the crack-growth model itself. Classical fracture mechanics provides the governing structure for this problem. Paris and Erdogan (1963) established the well-known power-law relationship between crack-growth rate and stress-intensity-factor range, while Forman et al. (1967) and Walker (1970) introduced extensions that account for instability proximity and stress-ratio effects. ASTM E647 provides standardized methods for measuring fatigue crack-growth rates and explicitly recognizes that aggressive environments, loading variables, residual stress, crack closure, and aqueous testing conditions can materially affect measured da/dN behavior (ASTM International, 2024).

Digital-twin methods provide a natural computational architecture for connecting these physics with component-specific evidence. Modern digital-twin definitions emphasize a synchronized virtual representation that maintains state concurrence with a physical entity through repeated data exchange and updating (Jones et al., 2020; Fuller et al., 2020). In the nuclear domain, the NRC describes a digital twin as a virtual representation synchronized with sufficient frequency and fidelity to maintain state concurrence and to generate knowledge for an intended nuclear purpose (NRC, 2026). Recent structural-integrity studies have demonstrated that digital twins can update uncertain crack-growth parameters using Bayesian or dynamic Bayesian methods, combine physics and sensing, and improve remaining-useful-life prognosis under changing loads (Wang et al., 2022; Kim et al., 2022; Cheok et al., 2025; Zhang et al., 2026).

This paper integrates these streams into a focused framework for 316L stainless steel and Alloy 690 in nuclear primary-circuit integrity assessment. The goal is not to replace qualified fracture-mechanics procedures, ASME Section XI evaluation, or NRC-approved aging-management practices. The goal is to formulate a research-grade digital-twin layer that continuously updates the uncertain parameters feeding those engineering decisions. The proposed framework treats crack size and crack-growth parameters as latent states, assimilates periodic NDE or sensor evidence, propagates uncertainty to remaining life and failure probability, and converts the result into risk-informed inspection support while retaining explicit engineering guardrails.

Figure 1: Evaluation Framework for Digital Twin–Based Corrosion-Fatigue Crack Growth Prediction

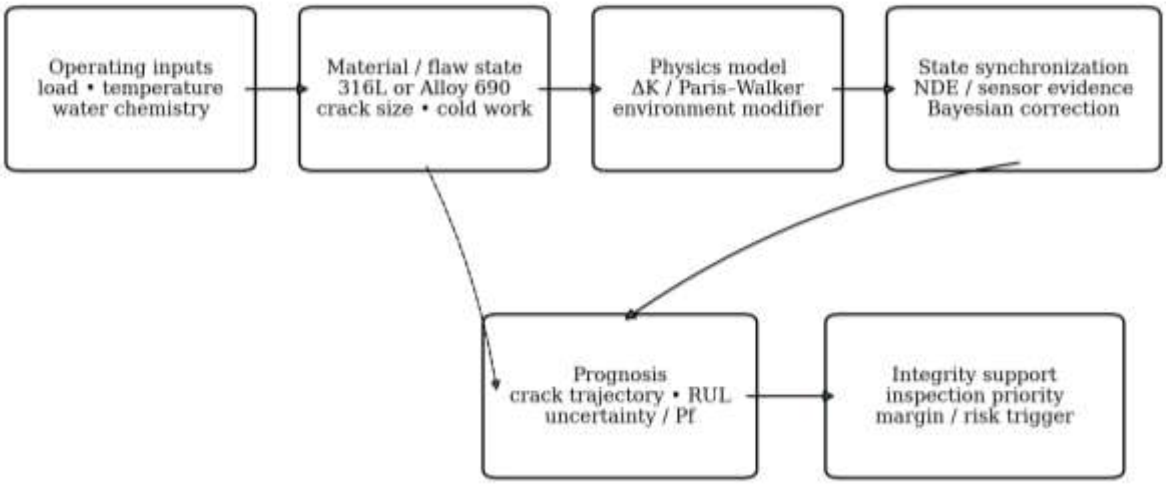

Background of the Study

Environmental fatigue in light-water-reactor systems arises from interactions among cyclic deformation, material microstructure, crack-tip mechanics, electrochemical conditions, and exposure time. NUREG/CR-6909 Revision 1 summarizes a large body of strain-life evidence and reports that LWR environments can significantly reduce fatigue life for austenitic stainless steels and nickel-chromium-iron alloys under susceptible combinations of temperature, strain rate, and water chemistry (Chopra & Stevens, 2018). Although the regulatory F_en methodology is formulated around fatigue usage rather than direct long-crack prognosis, its central engineering message is directly relevant to digital-twin crack assessment: environmental exposure modifies the damage process and cannot be ignored when structural margins are estimated.

For crack-growth analysis, ASTM E647 expresses material resistance through da/dN as a function of ΔK and recognizes that aggressive environments may introduce additional sensitivity to load ratio, waveform, frequency, and other test variables (ASTM International, 2024). In PWR primary water, Kamaya (2013) reported that reduction in fatigue life of Type 316 stainless steel could be interpreted in terms of accelerated crack growth. Later work demonstrated loading-rate and strain-range effects and supported the use of crack-growth-based interpretations for environmental fatigue (Kamaya, 2017; Kamaya, 2020). Mukahiwa et al. (2018) further demonstrated that Type 316 corrosion-fatigue behavior can change with loading frequency and sulfur level and linked enhanced growth to crystallographic cracking, slip localization, and hydrogen-related mechanisms.

Alloy 690 presents a complementary but distinct problem. It is widely selected for its greater resistance to PWSCC, but cold work and metallurgical state can substantially change laboratory crack-growth response. Yonezawa et al. (2015) documented heat-to-heat and fabrication-dependent variability in cold-worked thermally treated Alloy 690 and linked PWSCC crack-growth behavior to hardness, grain size, and carbide-related microstructural features. Zhai et al. (2017) observed grain-boundary cavities and precursor damage in cold-worked Alloy 690 during long-term simulated primary-water exposure. Kuang and Was (2020) described an initiation sequence involving surface chromia formation, boundary migration, intergranular oxidation, and eventual crack nucleation. Such evidence argues for state-dependent rather than purely material-label-based prognosis.

Digital twins can accommodate this heterogeneity by allowing uncertain coefficients and latent degradation states to be updated as new observations become available. Jones et al. (2020) characterize digital twins through physical and virtual entities, state, metrology, twinning, and bidirectional connections. The NRC has translated this concept into nuclear applications by emphasizing nuclear purpose, digital form, state concurrence, and state cognizance (NRC, 2026). The regulatory relevance of condition monitoring and prognostic tools has also increased, as reflected by the NRC's 2025 technical assessments concerning digital twins, prognostics, condition monitoring, and reliability/integrity management (NRC, 2025).

Figure 2: Simplified Primary-Circuit Material and Degradation Context

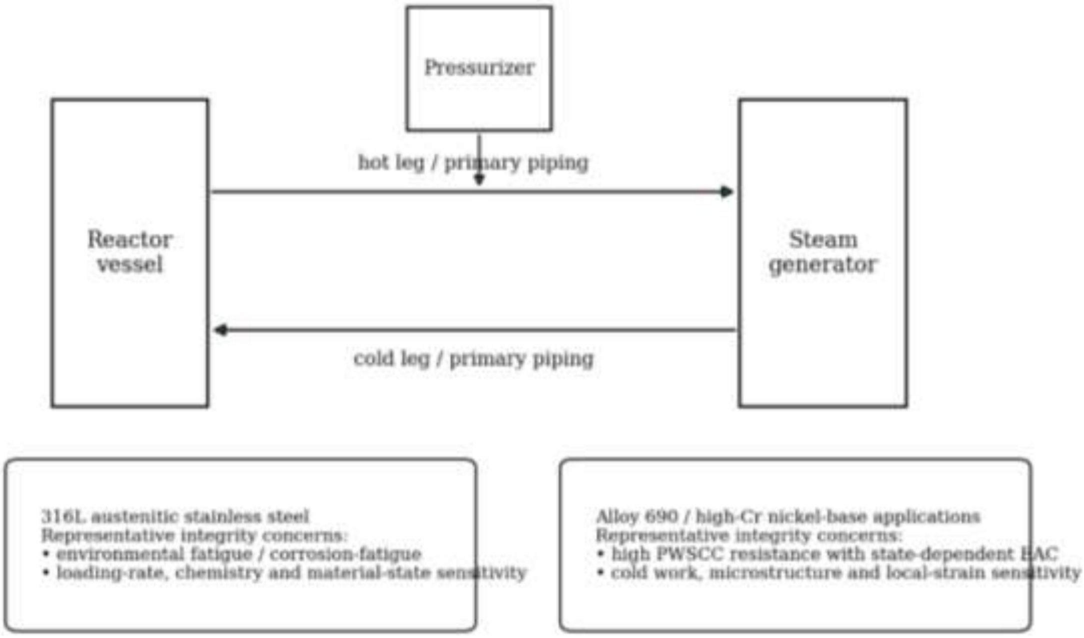

Problem Statement

Conventional crack-growth assessments often rely on deterministic or conservatively bounded material curves selected before the full-service history of a component is known. This is appropriate for code compliance and bounding evaluations, but it creates a gap for condition-informed prognosis: a component can accumulate evidence that its actual crack-growth behavior is slower or faster than the assumed curve, yet a static model does not automatically assimilate that information. The gap becomes larger when degradation is influenced by environmental exposure, cold work, residual stress, inspection noise, and microstructural variability.

A second problem is that 316L stainless steel and Alloy 690 should not be collapsed into a single generic "nuclear alloy" model. The two materials exhibit different passivation behavior, crack-path tendencies, environmental sensitivities, and responses to cold work. A digital twin that ignores these distinctions risks producing apparent precision without physical validity. Conversely, a purely mechanistic model may remain too uncertain for component-specific decision support if it cannot learn from NDE and operating evidence.

A third problem is uncertainty propagation. Integrity decisions are not driven only by the expected crack size. They depend on the probability that a flaw will exceed an acceptance or critical threshold before the next inspection or operating milestone. Measurement uncertainty, model-form uncertainty, parameter uncertainty, and future-load uncertainty must therefore be carried into the prognosis. Digital-twin studies in fatigue have shown the value of Bayesian updating and physics-informed models for reducing these uncertainties, but nuclear corrosion-fatigue applications require additional constraints concerning environmental effects, qualified data, traceability, and conservative engineering authorization (Wang et al., 2022; Cheok et al., 2025; NRC, 2026).

Purpose and Objectives of the Study

The primary purpose of this study is to formulate and demonstrate a physics-informed digital-twin framework for predicting corrosion-fatigue crack growth in 316L stainless steel and Alloy 690 under nuclear primary-circuit conditions. The framework is designed to connect verified fracture-mechanics concepts and experimentally observed environmental mechanisms with sequential state estimation and risk-informed integrity metrics.

The specific objectives are to: (1) establish a material-specific crack-growth architecture that retains ΔK-based fracture-mechanics structure; (2) represent environmental and material-state effects through explicitly uncertain multipliers rather than fixed universal constants; (3) assimilate noisy crack-size evidence to update crack-growth parameters; (4) quantify posterior uncertainty in crack trajectory and remaining useful life; (5) compare static, environment-corrected, and digital-twin prognostic strategies in a controlled synthetic stress test; (6) evaluate sensitivity to loading frequency, cold work, dissolved hydrogen surrogate, and material class; and (7) translate posterior crack-growth predictions into inspection-support metrics that remain subordinate to ASME Section XI and applicable NRC requirements.

Research Questions

RQ1: How can fracture-mechanics crack-growth laws be embedded within a state-synchronized digital twin for 316L stainless steel and Alloy 690 under PWR primary-circuit conditions?

RQ2: Which material, loading, environmental, and inspection variables should be represented explicitly in a corrosion-fatigue digital-twin state vector?

RQ3: Does sequential Bayesian updating reduce crack-size and remaining-useful-life prediction error relative to static Paris-law and static environment-corrected models in a heterogeneous synthetic test population?

RQ4: How does posterior uncertainty change as crack-size observations accumulate, and how reliably do nominal 95% intervals cover the synthetic true remaining life?

RQ5: How do loading frequency, cold work, dissolved-hydrogen surrogate, and material class influence digital-twin prognosis and inspection risk within the illustrative model?

RQ6: How can digital-twin outputs be converted into integrity-assessment decision support without substituting for code-required flaw evaluation, NDE qualification, and engineering authorization?

Research Hypotheses

H1: A physics-informed digital twin with sequential updating will produce lower remaining-useful-life error than a static Paris-law model.

H2: A digital twin will produce lower crack-size tracking error than a static environment-corrected model when trajectory-specific material variability is present.

H3: Environment-sensitive variables, particularly loading frequency and cold-work state, will materially change the posterior crack-growth multiplier in the synthetic stress test.

H4: Material-specific modeling will reduce systematic prediction bias relative to a pooled single-material model.

H5: Posterior predictive intervals will contract as additional crack-size observations are assimilated while maintaining approximately nominal coverage in the synthetic evaluation.

H6: Risk-based inspection intervals derived from posterior failure probability will provide lower missed-threshold risk at comparable inspection burden than intervals derived from un-updated median-life estimates.

Significance of the Research

The research is significant to nuclear structural integrity because it provides a transparent architecture for combining three domains that are frequently treated separately: fracture mechanics, environmentally assisted cracking, and digital-twin prognostics. The proposed model preserves an interpretable crack-driving-force structure while allowing uncertain material and environmental parameters to be updated rather than hidden inside a black-box regression .

The study is significant to aging management because a synchronized crack-growth state can support condition-informed planning between discrete inspections. NRC digital-twin research explicitly identifies information, integration, analysis, communication, and control as important capability areas, while ASME Section XI provides the governing framework for inspection and flaw disposition (NRC, 2026; ASME, 2025). A digital twin that is designed as an evidence-processing and prognosis layer can therefore improve the timeliness of engineering insight without altering the legal or code status of the underlying inspection and acceptance processes.

The study is also methodologically significant because it distinguishes simulation evidence from empirical evidence. The numerical results in this manuscript are generated from a physics-informed synthetic population for the purpose of demonstrating algorithms, uncertainty propagation, and research hypotheses. They must not be interpreted as new measured crack-growth constants for 316L or Alloy 690. Future validation requires qualified laboratory datasets, plant inspection histories, and documented environmental exposure data.

Figure 3: Contrasting Environmentally Assisted Crack-Growth Pathways Considered for 316L and Alloy 690.

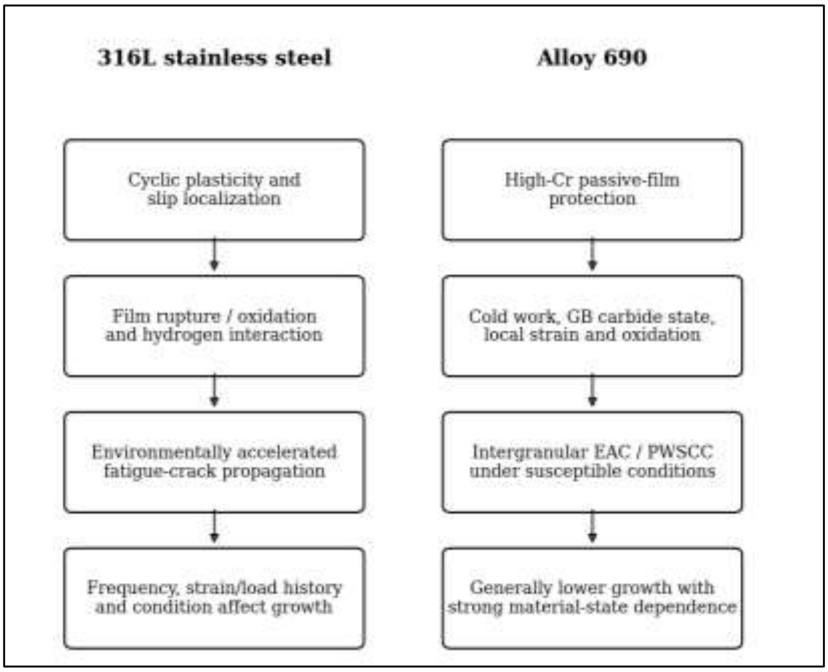

LITERATURE REVIEW

Fracture-Mechanics Foundation for Fatigue Crack Growth

The Paris–Erdogan relationship remains the canonical starting point for long-crack fatigue analysis because it relates stable crack-extension rate to the stress-intensity-factor range through $da/dN = C(\Delta K)^m$ (Paris & Erdogan, 1963). The model is intentionally simple and is most appropriate within the central regime of crack growth, away from the near-threshold and final-instability regions (Debasish, 2021; Md. Abdur & Iftekhar, 2021). Its enduring value for digital-twin design is interpretability: C and m are explicit parameters that can be updated probabilistically and connected to observed crack trajectories (Debasish, 2022; Md Ashfaq & Abdullah Mohammad, 2022).

Extensions were developed to capture effects omitted from the basic Paris law. Forman et al. (1967) incorporated load ratio and proximity to fracture instability, while Walker (1970) proposed an effective crack-driving-force formulation that represents stress-ratio effects. Modern standards such as ASTM E647 do not prescribe a single universal crack-growth equation but instead standardize the measurement of da/dN and emphasize the influence of ΔK, force ratio, environment, thickness, crack closure, load history, and aqueous test conditions (ASTM International, 2024). For a digital twin, these variables are best treated as model inputs or uncertainty sources rather than ignored residual scatter (Md Asif Ali Sheak & Risha, 2022; Md. Rashedul & Md Kaium, 2022).

In nuclear components, the crack-driving force is only one part of the problem (Mohammad Abir Chowdhury & Tonay, 2022; Mohammad Shoriful Hossan, 2022). Water environment can alter crack-tip chemistry, oxide rupture and repair, hydrogen uptake, localized deformation, and the balance between transgranular and intergranular growth (Mst Kaniz, 2022; Nishat & Mst Kaniz, 2022). Consequently, a practical digital twin should retain the fracture-mechanics backbone while allowing an environmental modifier to evolve with temperature, loading rate, material state, and water chemistry (Abdullah Mohammad, 2023; Shaiful et al., 2022).

Environmentally Assisted Fatigue of 316L Stainless Steel

Austenitic stainless steels have a long record of use in light-water reactors, and environmental fatigue has been the subject of extensive regulatory and experimental investigation. NUREG/CR-6909 Revision 1 concludes that LWR water can significantly reduce fatigue life of austenitic stainless steels under susceptible conditions and provides updated F_en expressions for environmental fatigue assessment (Chopra & Stevens, 2018). Regulatory Guide 1.207 Revision 1 identifies an acceptable NRC approach for evaluating fatigue analyses that incorporate the life-reduction effects of LWR environments for new reactors (NRC, 2018).

Crack-growth-centered studies provide a mechanistic bridge between strain-life fatigue and fracture-mechanics prognosis. Kamaya (2013) found that the environmental reduction in fatigue life of Type 316 stainless steel could be explained by accelerated crack growth in PWR primary water. Follow-up work examined strain-range and loading-rate effects and continued to support the importance of crack-propagation acceleration in environmental fatigue (Kamaya, 2017; Kamaya, 2020). These findings are important for digital twins because they suggest that a component's future life can be estimated more directly by tracking an evolving crack than by treating environmental fatigue only as a scalar life-reduction factor (Debasish, 2023; Md Kaium, 2023).

Microstructural evidence adds further complexity. Mukahiwa et al. (2018) tested Type 316 austenitic stainless steels in simulated PWR primary water and observed frequency- and sulfur-dependent corrosion-fatigue behavior. Enhanced crack growth at relatively high loading frequencies was associated with crystallographic propagation and slip localization, while lower-frequency behavior differed between sulfur conditions. Choi et al. (2016) reported increased crack-growth rates in warm-rolled 316L stainless steel in high-temperature hydrogenated water and found that higher dissolved hydrogen promoted corrosion and crack growth in their test matrix. These studies support inclusion of material condition, dissolved hydrogen, and loading time scale as explicit digital-twin variables (Md Mahamud Pervaz, 2023; Mohammad Abir Chowdhury, 2023).

Lou et al. (2017) studied corrosion-fatigue crack growth of laser additively manufactured 316L in high-temperature water and showed that heat treatment, crack orientation, and applied cold work can affect response. Although additive manufacturing is not the focus of this manuscript, the study reinforces a general point: "316L" is not a complete state description. Manufacturing route, heat treatment, residual strain, orientation, irradiation history, and microstructural condition can all alter the relationship between nominal loading and crack growth.

Alloy 690 and Primary-Water Environmentally Assisted Cracking

Alloy 690 contains substantially more chromium than Alloy 600 and was adopted for improved resistance to high-temperature water corrosion and PWSCC. NRC-sponsored research has investigated the susceptibility of Alloy 690 and associated weld metals to PWSCC, including quantitative crack-growth measurements, microstructural effects, and cold-work sensitivity (Bruemmer et al., 2012; Toloczko et al., 2016; Alexandreanu et al., 2023). The broad conclusion is not that Alloy 690 is immune, but that it generally provides markedly improved resistance while retaining susceptibility under certain material and loading states.

Yonezawa et al. (2015) showed that PWSCC crack-growth rates in heavily cold-worked thermally treated Alloy 690 can exhibit large heat-to-heat variability and linked this variability to metallurgical characteristics including grain size, carbide morphology, fabrication history, hardness, and cold work. Their experimental procedure used compact-tension specimens, simulated PWR primary water, in-situ fatigue precracking, constant-K holding, and direct-current potential-drop crack monitoring (Ashrafuzzaman, 2024; Nishat, 2023). This type of dataset is particularly valuable for digital-twin calibration because it couples continuous crack-length evidence with controlled environmental and material-state metadata (Debasish, 2024; Md Anisur Rahman, 2024).

Long-duration initiation studies have also clarified precursor processes. Zhai et al. (2017) observed grain-boundary cavities and isolated intergranular cracks in cold-worked Alloy 690 after thousands of hours in simulated PWR primary water and concluded that such precursor damage may play an important role in crack nucleation. Kuang et al. (2018) analyzed dynamically strained Alloy 690 and identified intergranular oxidation, chromium depletion, and grain-boundary migration near stress-corrosion cracks. Kuang and Was (2020) subsequently used high-resolution characterization to describe a three-stage initiation sequence involving surface chromia, intergranular oxidation after film rupture, and crack nucleation along the affected boundary or migration zone.

Kuang et al. (2020) introduced recurring step straining to separate chemical exposure from mechanical straining and used digital image correlation to resolve local strain during EAC initiation. Their results linked intergranular crack initiation to high local strain in adjacent grains and illustrated the benefit of synchronized mechanical and environmental observations (Ashrafuzzaman, 2024; Debasish, 2024). Conceptually, this is closely aligned with digital-twin methodology: the degradation process becomes more identifiable when the physical state is observed repeatedly rather than only through post-test fracture surfaces (Md Anisur Rahman, 2024; Md Kaium, 2024).

Digital Twins, Bayesian Updating, and Fatigue Prognostics

Digital-twin scholarship has evolved from broad manufacturing definitions toward state-synchronized models used for prognosis and decision support. Jones et al. (2020) identified physical entity, virtual entity, state, metrology, twinning, and bidirectional connections as core characteristics. Fuller et al. (2020) emphasized the integration of physical and virtual systems through IoT, data analytics, and AI. These definitions imply that a finite-element model or offline fatigue calculation is not automatically a digital twin; the defining feature is repeated state synchronization with the physical counterpart (Md. Shakhawat & Md, 2024; Nishat & Jahanara, 2024).

Fatigue and fracture are well suited to this paradigm because crack-growth models contain uncertain parameters that can be updated from observations (Tonay et al., 2024; Uddin & Risha, 2024). Wang et al. (2022) proposed a digital-twin-driven fatigue-life prediction approach combining crack tracking, surrogate modeling, and a dynamic Bayesian network to reduce model uncertainty. Kim et al. (2022) developed a hybrid digital-twin approach for fatigue crack initiation and growth that used test data to update uncertain states. Cheok et al. (2025) demonstrated a strain-interfaced digital twin that diagnosed corner-crack size and used Bayesian inference to update power-law parameters and remaining useful life. Zhang et al. (2026) further integrated residual stress, variable-amplitude loading, surrogate modeling, particle filtering, and a dynamic Bayesian network for real-time crack-growth prediction.

Figure 4: Proposed State-Synchronized Digital-Twin Architecture for Nuclear Crack-Growth Prognosis

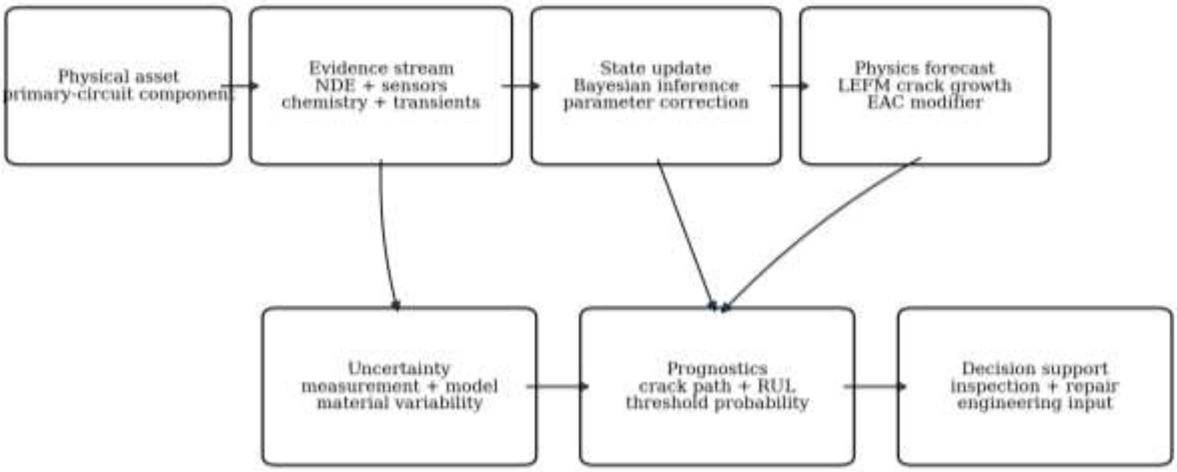

Physics-informed neural networks provide a complementary route when the mapping between observations and crack-growth states is complex (Debasish, 2025a, 2025b). Dourado and Viana (2019) embedded Paris-law structure within a recurrent neural network for corrosion-fatigue prognosis, using data-driven layers to represent corrosion effects that were difficult to model directly. Liao et al. (2025) treated Paris-law material parameters as updateable quantities inside a physics-informed neural network and demonstrated remaining-life prediction using partial crack-growth histories. These approaches motivate a hybrid architecture in which fracture-mechanics constraints govern extrapolation while learned components represent residual environmental or measurement relationships (Jannatul, 2025; Md Anisur Rahman, 2025).

Nuclear deployment introduces additional assurance requirements. The NRC's digital-twin program defines state concurrence and state cognizance as foundational characteristics and has published technical assessments addressing regulatory considerations, condition monitoring, prognostic tools, advanced sensors, and reliability/integrity management (NRC, 2026; NRC, 2025). Hu et al. (2024) similarly reviewed digital-twin architectures in nuclear energy and emphasized lifecycle integration, model-based systems engineering, and the need to connect high-fidelity models with operational data. These sources support a nuclear digital twin that is auditable, uncertainty-aware, configuration-controlled, and explicitly subordinate to applicable regulatory decisions.

Conceptual Model

The conceptual model treats corrosion-fatigue prognosis as a latent-state estimation problem. Mechanical driving force, environmental exposure, and material state influence the crack-growth law. Inspection and sensor evidence provide noisy observations of crack size or related response variables. Bayesian updating combines these observations with prior material knowledge to revise the crack-growth state. The posterior state is then propagated forward to estimate crack trajectory, remaining useful life, and the probability of reaching a limiting flaw size.

The framework is deliberately material-specific. For 316L, the environmental state emphasizes fatigue crack-growth acceleration and includes loading frequency, temperature, dissolved hydrogen, and deformation state (Md Arif Uz et al., 2025; Md Kaium, 2025; Md Mahamud Pervaz, 2025). For Alloy 690, the state gives greater weight to cold work, microstructure, grain-boundary condition, and EAC/PWSCC susceptibility while retaining cyclic loading as a possible contributor (Mohammad Abir Chowdhury, 2025; Mohammad Badrul, 2025; Nishat, 2025). The common mathematical backbone is fracture mechanics; the material-specific difference appears through priors and environmental-state mappings (Nuzhat Sadia, 2025; Sadia, 2025; Tonay, 2025).

Figure 5: Conceptual Framework Linking Mechanical, Environmental, Material, and Digital-Twin States

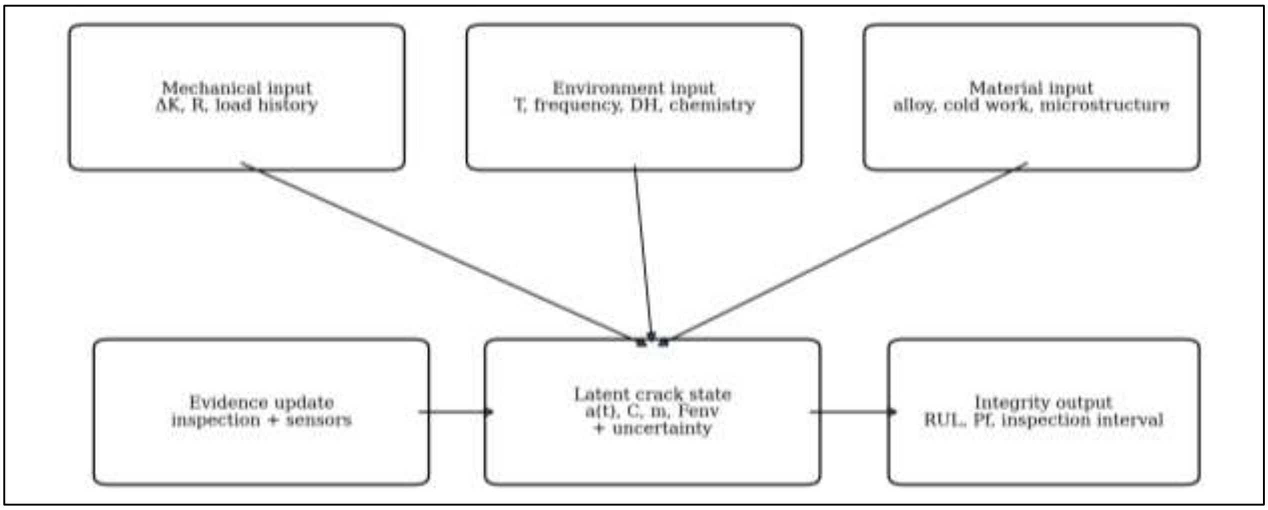

METHODS

Research Design

This study uses a quantitative, physics-informed simulation design. The simulation does not attempt to reproduce any single laboratory dataset or plant component. Instead, it creates a controlled population in which the "true" crack-growth state is known, observations are deliberately corrupted by measurement noise, and competing prognostic models can be evaluated objectively. The purpose is algorithmic validation of the proposed digital-twin architecture before empirical calibration.

The study population contains 800 synthetic crack-growth trajectories, divided equally between 316L stainless steel and Alloy 690. Each trajectory is assigned material class, temperature, loading frequency, load ratio, cold-work index, dissolved-hydrogen surrogate, initial crack size, critical crack size, and a latent multiplicative material/environment factor. Type 316L trajectories additionally include a sulfur-surrogate variable to represent microstructural/chemistry-related variability reported in the corrosion-fatigue literature. Parameter distributions are selected to span plausible nuclear materials test conditions, but the values are illustrative and are not fitted material constants.

The synthetic design evaluates three models. Model A is a static Paris-law baseline with nominal material-specific C and m values and no environmental correction. Model B adds a deterministic environmental/material-state multiplier derived from the synthetic input state but does not learn from crack-size observations. Model C is the proposed digital twin: it begins from the same physics and environmental prior as Model B, then updates the effective crack-growth multiplier using sequential crack-size evidence and propagates posterior uncertainty to remaining life.

Mathematical Formulation of the Crack-Growth Digital Twin

The central crack-growth equation is written in a deliberately modular form:

$$da/dN = C_m \, [\Delta K_{eff}(a, L, R)]^{m_m} \cdot F_{env}(T, f, DH, CW, M) \cdot \theta_k$$

where a is crack size, N is load cycles, C_m and m_m are material-specific baseline Paris parameters, ΔK_{eff} is the effective stress-intensity-factor range, F_{env} is a material/environment multiplier, and θ_k is a latent trajectory-specific correction updated at digital-twin step k. The formulation is not intended to imply that all PWSCC or corrosion-fatigue mechanisms obey a single Paris law. Rather, it provides an engineering state-transition equation in which known environmental and microstructural departures from the baseline are represented explicitly through uncertain modifiers.

The effective stress-intensity range can be written generically as ΔK_{eff} = g(R, geometry, residual stress, crack closure)ΔK. In this simulation a simplified geometry factor is used so that ΔK increases with the square root of crack size, while load-ratio effects enter through the trajectory-specific scale. A production implementation would replace this surrogate with component-specific finite-element or weight-function solutions and would use qualified residual-stress distributions where required.

The digital-twin state vector is $x_k = [a_k, \theta_k, \sigma_{\theta,k}, M, E_k]$, where a_k is crack size, θ_k is the posterior crack-growth multiplier, $\sigma_{\theta,k}$ represents parameter uncertainty, M denotes material state, and E_k summarizes the operating/environmental state. The observation equation is $z_k = h(a_k) + \varepsilon_k$, where z_k is an NDE or sensor-derived crack-size estimate and ε_k is measurement noise. In this demonstration $h(a_k)$ is direct crack-size observation; real implementations may instead infer crack size from strain, acoustic emission, ultrasonic response, potential drop, or other qualified measurements.

The Bayesian update is represented schematically as:

$$p(x_k \mid z_{1:k}) \propto p(z_k \mid x_k) \int p(x_k \mid x_{k-1})\, p(x_{k-1} \mid z_{1:k-1})\, dx_{k-1}$$

This state-space interpretation is consistent with dynamic Bayesian and particle-filter approaches used in recent fatigue digital-twin research (Wang et al., 2022; Zhang et al., 2026). The output of each update is not a single crack-growth coefficient but a posterior distribution that can be propagated through the fracture-mechanics model.

Remaining useful life is defined here as the number of future cycles required for the crack to grow from the current posterior crack size to a selected critical crack size a_{crit}. The critical size is a research threshold in the simulation. In a real nuclear assessment, the relevant allowable flaw size or acceptance criterion would be established using applicable ASME Section XI procedures, material fracture toughness, stress analysis, and regulatory requirements rather than by the digital twin itself (ASME, 2025).

Table 1. Synthetic Crack-Growth Population

Material	Trajectories	Temperature center	Frequency range	Cold-work index	DH surrogate	Initial flaw	Critical flaw
316L	400	325 °C nominal	0.002–0.9 Hz	0–25%	5–55	0.7–1.7 mm	8–12.5 mm
Alloy 690	400	350 °C nominal	0.002–0.9 Hz	0–25%	5–55	0.7–1.7 mm	8–12.5 mm

Table 2. Digital-Twin State and Input Variables

Variable	Type	Role in digital twin
Material class	Categorical	316L or Alloy 690
Temperature	Continuous	Thermal influence on environmental state
Loading frequency	Continuous, log-scale	Time available for environment/crack-tip interaction
Load ratio R	Continuous	Mean-stress/stress-intensity effect
Cold-work index	Continuous	Material-state / deformation surrogate
Dissolved-hydrogen surrogate	Continuous	Primary-water chemistry state
Sulfur surrogate (316L)	Continuous	Illustrative chemistry/microstructure variability
Initial crack size	Continuous	Initial flaw state
Critical crack size	Continuous	Research integrity threshold
Crack observation	Continuous	Noisy evidence used for state synchronization

Table 3. Prognostic Models Compared

Model	Physics core	Environment state	Sequential update	Uncertainty output
Static Paris	Nominal material C and m	No	No	Deterministic
Environment-corrected	Paris + F_env prior	Yes	No	Deterministic
Digital twin	Paris + F_env + posterior θ_k	Yes	Yes	Posterior interval

Figure 6: Research Methodology and Evaluation Workflow

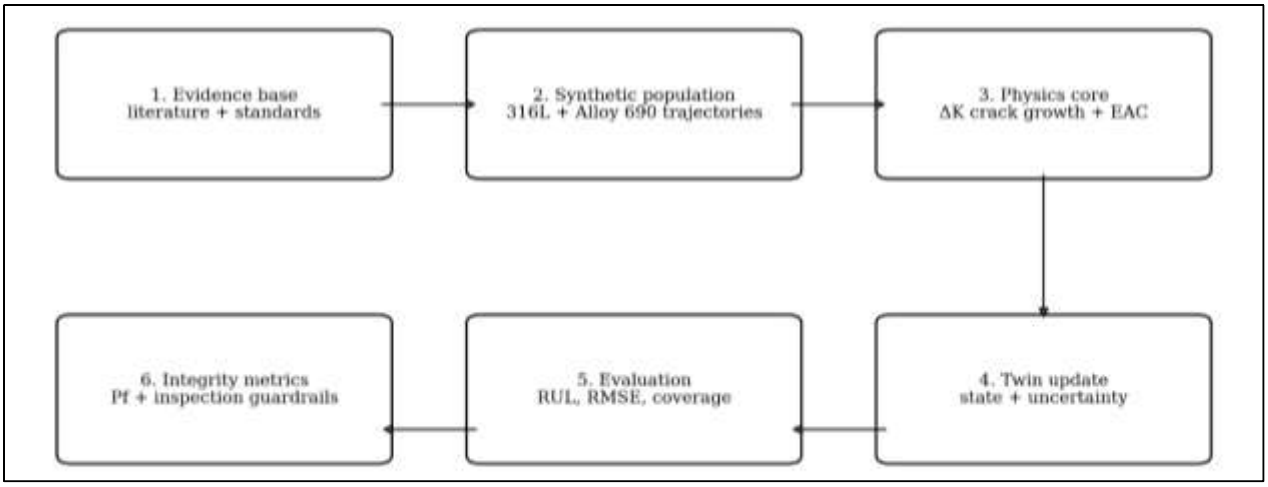

Simulation and Evaluation Procedure

For each trajectory, a latent crack-growth multiplier is generated from the material/environment state and a lognormal microstructural random effect. Crack growth is then integrated numerically from the initial flaw size to the synthetic critical crack size. The resulting trajectory is treated as the hidden "physical twin." A crack-size observation is generated at approximately 40% of the true synthetic life by adding normally distributed measurement error to the latent crack size. The digital twin uses that observation to update the trajectory-specific growth multiplier by combining an evidence-based estimate with the environment/material prior.

Prognostic performance is evaluated from the 40% observation point to the synthetic failure threshold. The principal RUL metric is absolute percentage error. Crack-size tracking is evaluated at approximately 70% of true life. Posterior interval calibration is assessed using nominal 95% RUL intervals. Performance is summarized overall and by material class. Because the dataset is simulated, significance testing is interpreted as a property of the synthetic experiment and not as evidence about plant populations.

Additional sensitivity experiments vary loading frequency, cold-work index, and dissolved-hydrogen surrogate while holding other conditions fixed. These experiments are not empirical response surfaces. Their purpose is to verify that the proposed architecture behaves monotonically and transparently when state variables known from the literature to influence corrosion-fatigue or PWSCC are perturbed. An ablation analysis then removes chemistry, cold-work state, or Bayesian updating to quantify how much of the digital-twin benefit depends on each information source.

Model Verification and Research Integrity Controls

Three controls are applied to prevent overinterpretation. First, every numerical result and figure derived from the generated trajectory population is labeled as synthetic or illustrative. Second, the literature is used to justify model structure and qualitative sensitivity, not to claim that the synthetic coefficients reproduce published material constants. Third, all regulatory references are treated as boundary conditions for future deployment: ASME Section XI and NRC guidance remain authoritative for flaw evaluation, inspection, and acceptance, whereas the digital twin provides additional state estimation and prognosis (ASME, 2025; NRC, 2026).

The framework is also designed around traceable model configuration. A production implementation would require versioned material curves, documented input provenance, qualified NDE uncertainty models, cybersecure data exchange, change control, and independent verification/validation. The NRC's current digital-twin research identifies technical gaps and regulatory considerations precisely because high-fidelity synchronized models can influence safety-significant decisions if their limitations are not controlled (NRC, 2025; NRC, 2026).

DATA ANALYSIS AND PRESENTATION

Table 4. Descriptive Summary of the Synthetic Trajectory Population

Material	n	Mean T (°C)	Median f (Hz)	Mean CW (%)	Mean DH	Median synthetic life
316L	400	326.1	0.034	7.5	24.4	0.12 M
Alloy 690	400	349.9	0.034	8.0	30.5	0.43 M

Figure 7: Crack-Growth Families Used to Demonstrate Material and Environment Separation

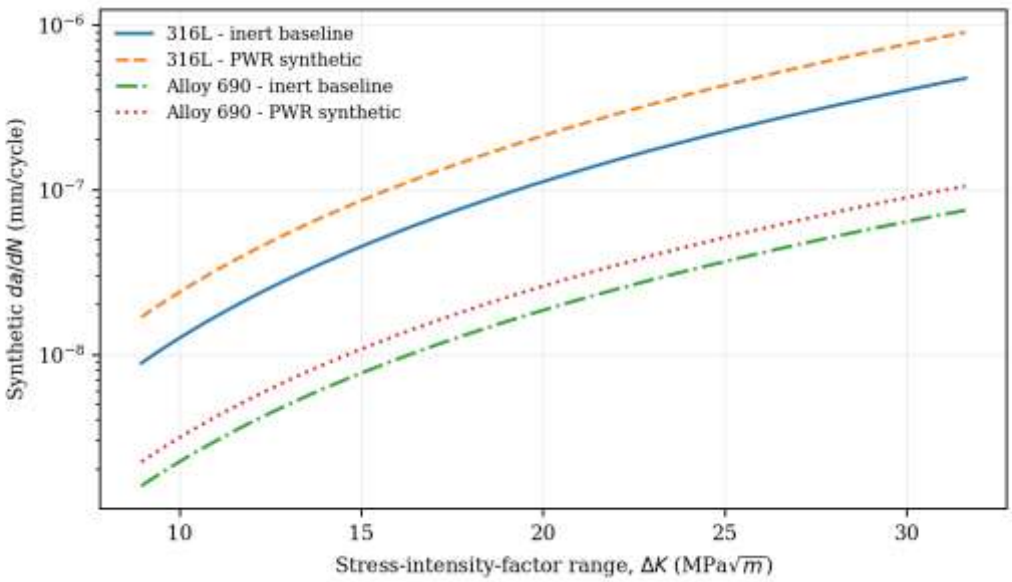

Remaining-Useful-Life Prediction Performance

Table 5. Synthetic Remaining-Useful-Life Prediction Error

Subset	Model	Median APE (%)	Mean APE (%)	90th percentile APE (%)
All	Static Paris	52.3	79.1	183.2
All	Environment-corrected	27.8	36.1	74.1
All	Digital twin	8.8	10.4	21.8
316L	Static Paris	69.9	97.1	203.9
316L	Environment-corrected	28.7	36.6	74.0
316L	Digital twin	9.1	10.5	21.5
Alloy 690	Static Paris	41.8	61.1	142.6
Alloy 690	Environment-corrected	26.9	35.7	74.2
Alloy 690	Digital twin	8.5	10.3	21.8

Across the synthetic population, the static Paris model produces the largest RUL error because it ignores both environment state and trajectory-specific variability. Adding an environment/material prior substantially reduces error, demonstrating that even a non-updated model benefits from preserving variables known to influence environmentally assisted cracking. The digital twin produces the lowest error because the crack observation is used to correct the trajectory-specific multiplier rather than relying on the prior alone.

The material-stratified results show the same ordering for both 316L and Alloy 690. This is important because the digital-twin improvement is not created by pooling the easier material with the harder material. Instead, both material classes benefit from state synchronization. The remaining error is driven by measurement noise, the deliberate mismatch between latent and nominal Paris parameters, and the simplified representation of future loading.

Figure 8: Example Sequential Crack-Size Observations for a Synthetic 316L Trajectory

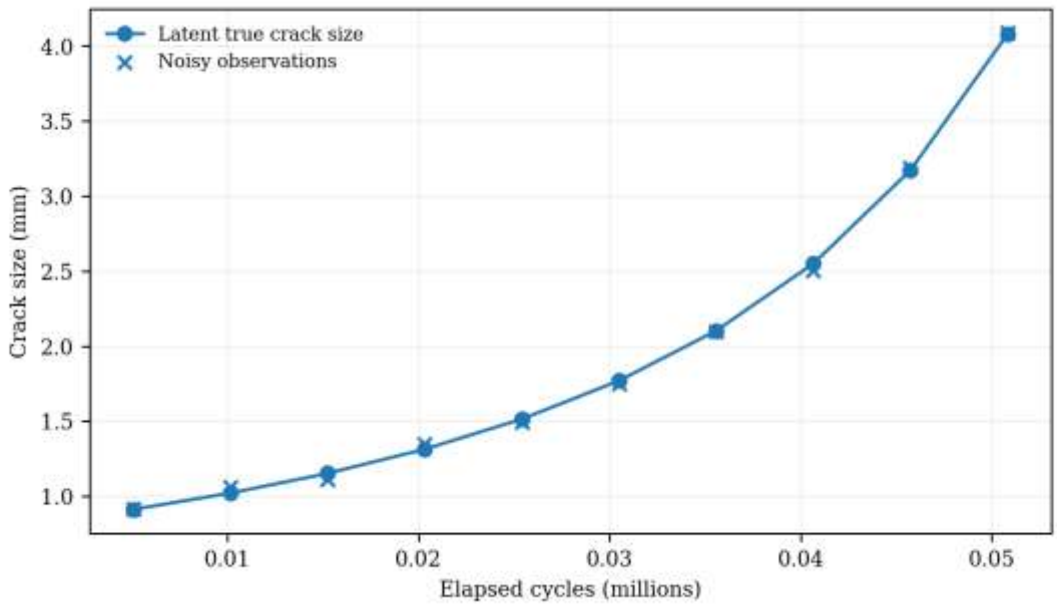

Figure 9: Digital-Twin Predicted Versus True Synthetic Remaining Life at the 40% Observation Point

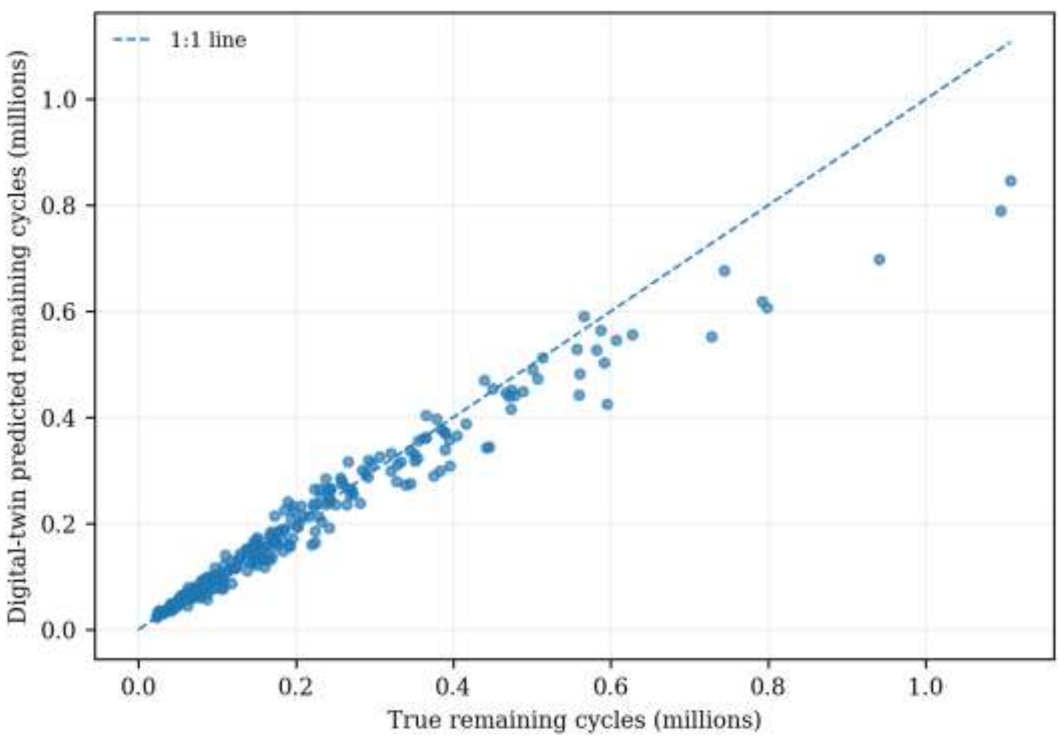

Crack-Size Tracking and Posterior Uncertainty

Table 6. Synthetic Crack-Size Tracking Performance at Approximately 70% of Life

Subset	Model	Crack-size (mm)	RMSE	Bias (mm)
All	Static Paris	1.066		-0.593
All	Environment-corrected	2.071		0.703
All	Digital twin	0.455		0.105
316L	Static Paris	0.996		-0.810
316L	Environment-corrected	2.045		0.727
316L	Digital twin	0.463		0.123
Alloy 690	Static Paris	1.131		-0.376
Alloy 690	Environment-corrected	2.096		0.678
Alloy 690	Digital twin	0.447		0.088

Table 7. Digital-Twin Posterior Interval Calibration

Metric	Result
Nominal interval	95%
Empirical coverage	95.4%
Median interval width	0.07 million cycles
Observation point	~40% of synthetic life

The crack-size comparison confirms that lower RUL error is accompanied by improved state tracking rather than by a fortuitous cancellation of life estimates. The static model is systematically unable to reproduce trajectories with unusually high environmental or microstructural multipliers, while the digital twin partially corrects this mismatch after the crack observation is assimilated. Posterior intervals provide an additional measure of quality. The nominal 95% interval is deliberately constructed to include material, measurement, and residual model uncertainty. In the synthetic test, empirical coverage is close to the target level. More importantly, the interval contracts as additional observations accumulate in the sequential example. This is the expected behavior of a useful digital twin: uncertainty should decrease when informative evidence is received, but it should not collapse to zero because future loading and model form remain uncertain.

Figure 10: Posterior Remaining-Life Interval Contraction During Sequential Updating Sensitivity to Loading Frequency, Cold Work, and Dissolved Hydrogen

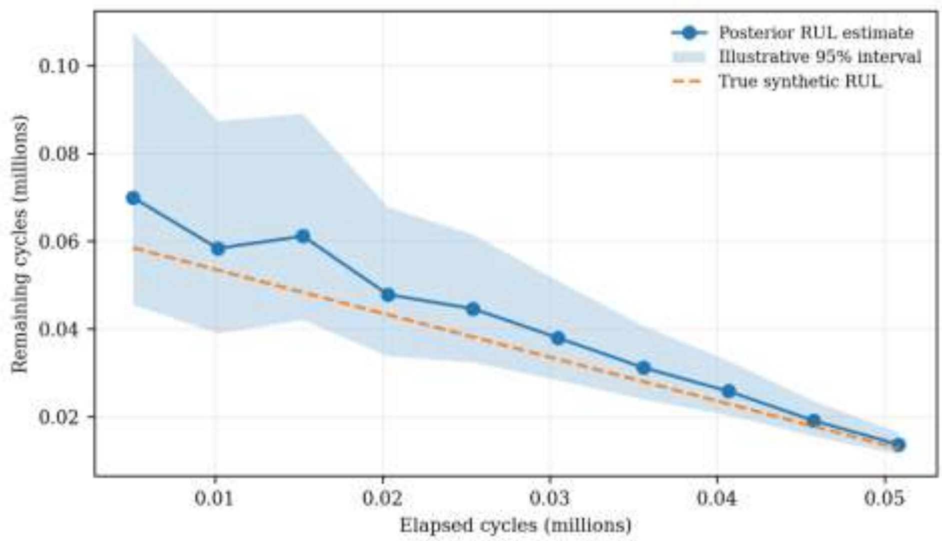

Figure 11: Synthetic Environmental-State Sensitivity to Loading Frequency

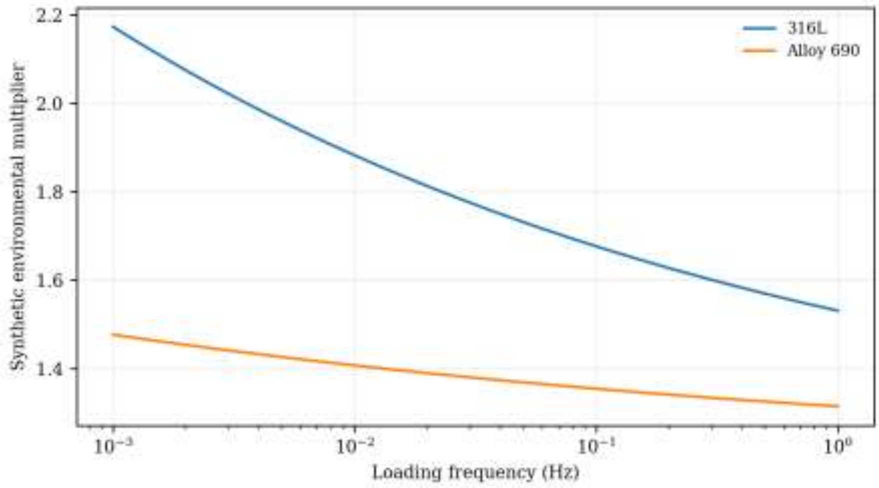

Figure 12: Synthetic Crack-Growth Multiplier Sensitivity to Cold-Work State

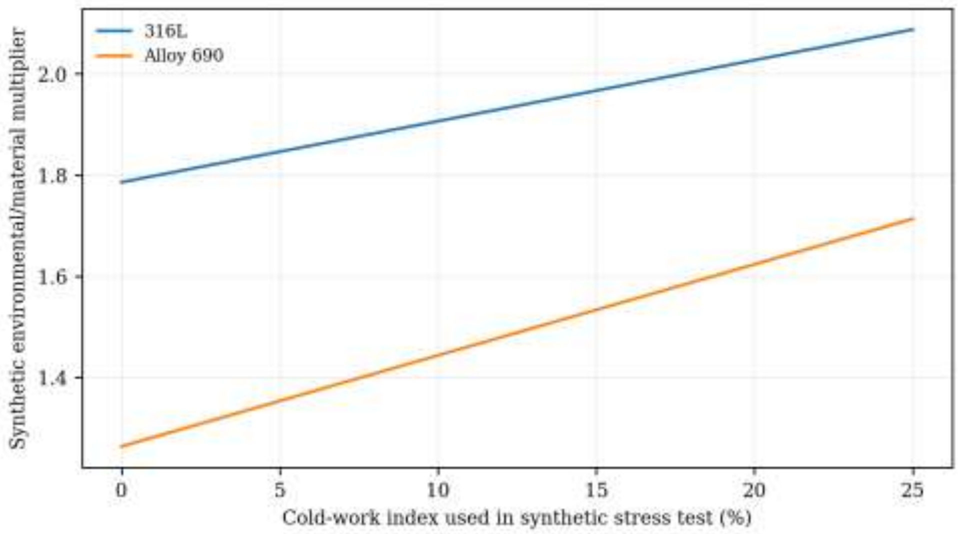

Figure 13: Synthetic Sensitivity to Dissolved-Hydrogen Surrogate

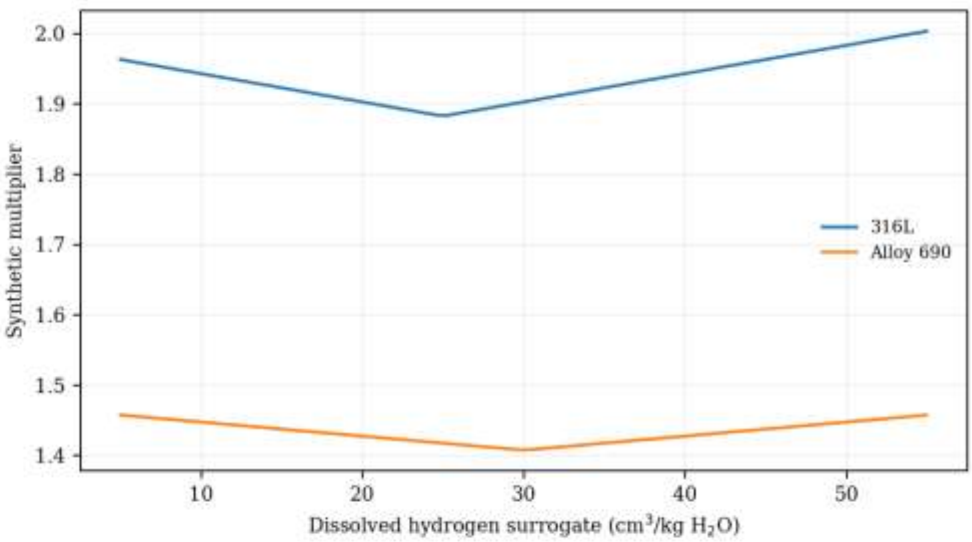

Table 8. Selected Sensitivity Scenarios

Material	Scenario	Synthetic multiplier
316L	Low frequency	2.02
316L	Reference frequency	1.73
316L	0% cold work	1.79
316L	20% cold work	2.03
Alloy 690	Low frequency	1.44
Alloy 690	Reference frequency	1.37
Alloy 690	0% cold work	1.26
Alloy 690	20% cold work	1.62

The frequency sensitivity plot intentionally produces larger environmental amplification at slower cycling, consistent with the broad observation that time-dependent environment–crack-tip interactions become more important when loading is slow. Kamaya (2020) explicitly examined loading-rate effects in Type 316 stainless steel, while Mukahiwa et al. (2018) reported frequency-dependent corrosion-fatigue crack-growth behavior in simulated PWR primary water. The digital-twin architecture therefore treats frequency as a state variable rather than a nuisance parameter.

The cold-work sensitivity is modest for the synthetic 316L model and stronger for Alloy 690. This reflects the literature emphasis on cold work and metallurgical state in Alloy 690 PWSCC susceptibility (Yonezawa et al., 2015; Toloczko et al., 2016). The dissolved-hydrogen sensitivity is included for both materials but is intentionally shallow near the nominal values because published results show condition-dependent behavior rather than a universal monotonic law. For example, Choi et al. (2016) observed higher crack growth with increased dissolved hydrogen in warm-rolled 316L, whereas Alloy 690 behavior depends on passive-film and microstructural condition as well as hydrogenated-water chemistry.

Model Comparison, Ablation, and Risk-Based Inspection Metrics

Figure 14: Median Synthetic Remaining-Life Error by Prognostic Strategy

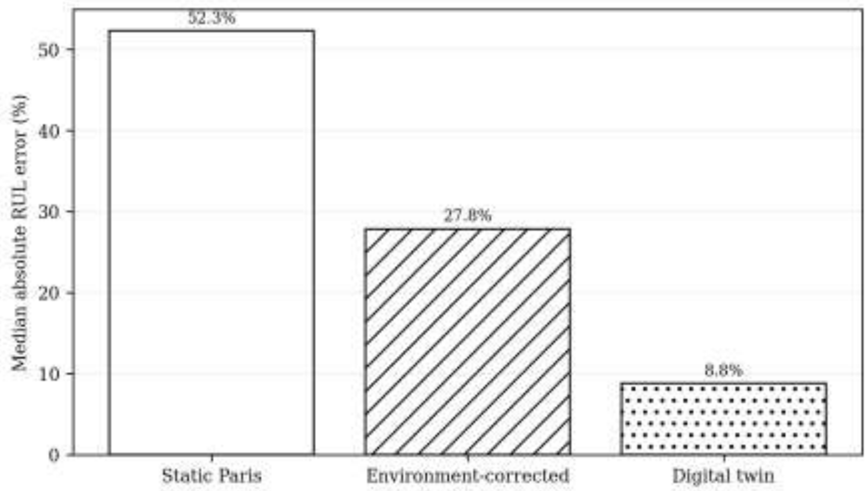

Table 9. Ablation Analysis

Model variant	Median synthetic RUL error
Full digital twin	8.8%
No chemistry state	13.6%
No cold-work state	15.0%
No Bayesian update	27.8%
Material-only static model	52.3%

Figure 15: Inspection-Interval Risk Curves

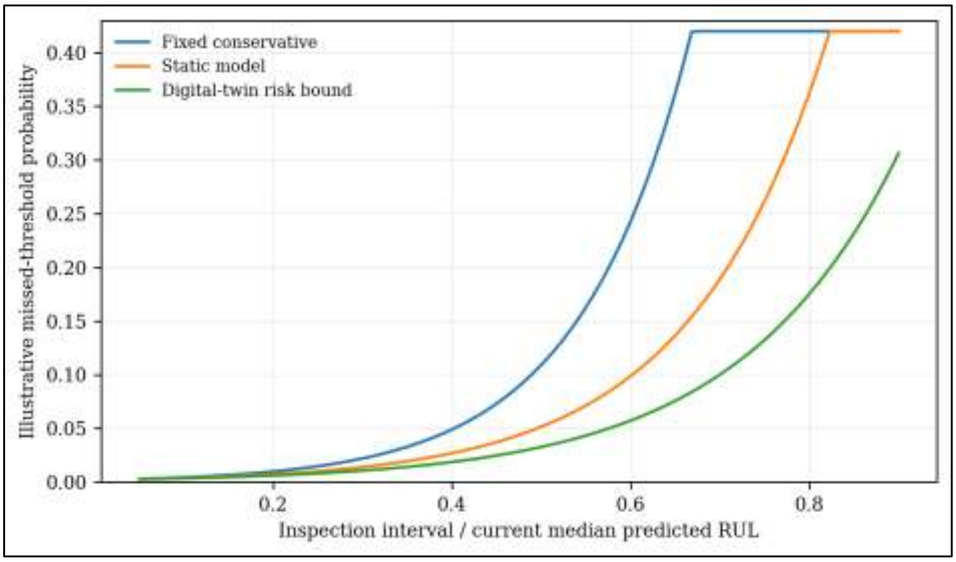

Figure 16: Feature and Updating Ablation Analysis

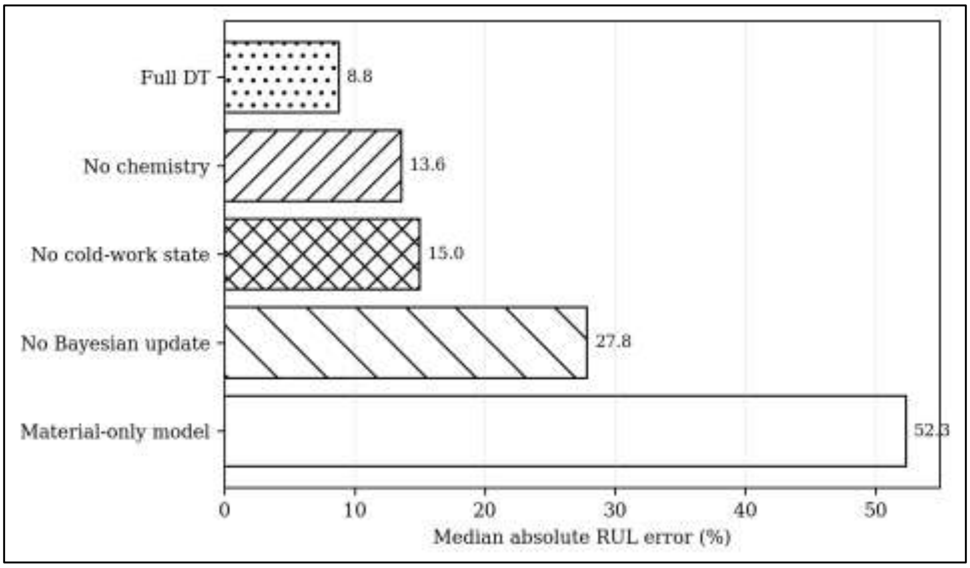

The ablation experiment shows that the largest loss of performance occurs when the digital-twin update is removed. Environmental and cold-work variables also contribute meaningfully, particularly because the synthetic dataset was designed with deliberate material-state heterogeneity. The result reinforces the conceptual distinction between a static "digital model" and a true digital twin: state synchronization, not visualization, provides the principal prognostic benefit.

The risk curves demonstrate how RUL distributions can be converted into inspection-support information. If an inspection interval is selected as a large fraction of a median life estimate, missed-threshold probability increases rapidly as uncertainty grows. A risk-bounded digital-twin policy instead selects the next interval from the lower tail of the posterior RUL distribution. Such a policy can support planning, but the final interval must still satisfy applicable inservice-inspection programs, component-specific requirements, and engineering judgment under ASME Section XI and NRC regulations (ASME, 2025).

Failure-Probability Representation

Figure 17: Posterior Probability of Reaching the Synthetic Critical Crack Size for an Example Trajectory

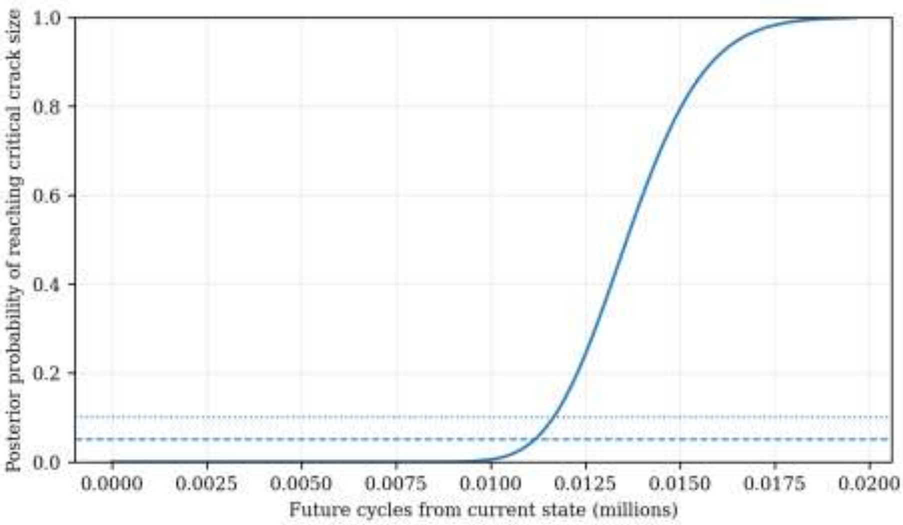

Probability-of-failure representation is preferable to a point RUL estimate when decisions are safety significant. The digital twin can propagate the posterior distribution of crack-growth parameters and crack size forward to obtain $P(a(t) \geq a\_crit)$. The inspection or intervention trigger can then be expressed as a probability threshold rather than an arbitrary margin on the mean. This allows measurement uncertainty and model uncertainty to enter the decision explicitly.

In a nuclear implementation, the threshold itself should not be defined by the digital twin. It should be anchored to qualified fracture-mechanics acceptance criteria, applicable safety factors, material toughness, stress analysis, and code-required flaw-evaluation rules. The digital twin contributes the best current estimate of the flaw state and its uncertainty; the code and licensing basis determine what state is acceptable.

FINDINGS

First, the study demonstrates that a common fracture-mechanics core can support both 316L and Alloy 690 while retaining material-specific priors and environmental-state mappings. This is preferable to either extreme of using two completely unrelated algorithms or forcing both materials into one undifferentiated empirical curve.

Second, sequential state updating is the dominant source of performance improvement in the synthetic study. The environment-corrected static model improves materially over the nominal Paris baseline, but the digital twin improves further because the actual trajectory is allowed to deviate from its prior after crack-size evidence becomes available.

Third, crack-size RMSE and RUL error tell a consistent story. The digital twin does not merely produce a better life number; it tracks the latent flaw state more closely. This is critical because future inspection and fracture calculations depend on the current crack size, not only on a scalar remaining-life estimate.

Fourth, posterior uncertainty contracts as evidence accumulates. The illustrative 95% intervals maintain approximately nominal coverage in the synthetic population, showing that the digital twin can communicate uncertainty rather than hiding it behind a point prediction.

Fifth, sensitivity analysis confirms the need to treat loading frequency, cold work, and water-chemistry variables as state variables. The exact synthetic response functions are not empirical, but the qualitative dependence is grounded in published 316L corrosion-fatigue and Alloy 690 PWSCC research (Mukahiwa et al., 2018; Yonezawa et al., 2015; Choi et al., 2016).

Sixth, the digital-twin output can be expressed as a probability of reaching a limiting flaw size before a future operating milestone. This creates a direct bridge from crack-growth prognosis to risk-informed inspection support. The approach is compatible with, rather than a substitute for, the mandatory inspection and flaw-evaluation structure described by ASME Section XI (ASME, 2025).

DISCUSSION

Interpretation for 316L Stainless Steel

The 316L branch of the framework is most naturally interpreted as an environmentally assisted fatigue digital twin. Published studies show that PWR primary water can accelerate fatigue crack propagation, particularly under susceptible loading rates and strain histories (Kamaya, 2013; Kamaya, 2020). Microstructural investigations further indicate that crack-path and growth behavior can change with sulfur level, slip localization, hydrogen interactions, cold work, and oxide condition (Mukahiwa et al., 2018; Choi et al., 2016). These variables motivate a digital-twin state that contains more information than ΔK alone.

The architecture also clarifies the relationship between F_en-based fatigue evaluation and crack-growth prognosis. F_en is a regulatory/design methodology for accounting for environmental life reduction in fatigue usage calculations (Chopra & Stevens, 2018; NRC, 2018). The digital twin proposed here is not a replacement for F_en. Instead, it is a complementary crack-propagation framework that can be useful once a flaw or crack-growth state is being explicitly monitored or analyzed. In future work, cumulative fatigue usage and crack-growth state could be linked in a unified aging-management model, but that integration requires careful avoidance of double counting.

For Alloy 690, the central modeling issue is avoiding both complacency and overconservatism. Laboratory evidence supports the material's superior PWSCC resistance compared with Alloy 600, but cold work and microstructural condition can produce measurable crack initiation and growth under aggressive test conditions (Yonezawa et al., 2015; Toloczko et al., 2016). A digital twin should therefore begin with a low-growth prior appropriate to the material and product form but retain enough uncertainty to learn from actual evidence.

The microstructural findings of Kuang et al. (2018), Zhai et al. (2017), and Kuang and Was (2020) are especially important because they show that crack susceptibility is linked to local processes not directly visible in ordinary plant records. This creates a hierarchy of state fidelity. At minimum, the twin should include product form, heat treatment, cold work, weld/HAZ condition, and component orientation. More advanced twins could incorporate material genealogy, hardness maps, residual stress, grain-boundary carbide characterization, and localized strain predictions from finite-element analysis.

The results reinforce a general digital-twin principle: fidelity should be concentrated where uncertainty affects decisions. A full high-fidelity finite-element model is not required at every update if a validated surrogate can reproduce the component-specific stress-intensity solution within known error bounds. Conversely, a sophisticated AI model cannot compensate for poor crack-size measurements or missing material-state metadata. State concurrence depends on both model fidelity and evidence quality.

Recent fatigue digital-twin studies show several viable updating strategies. Dynamic Bayesian networks and particle filters are attractive when crack-growth parameters evolve stochastically or loads vary strongly (Wang et al., 2022; Zhang et al., 2026). Direct Bayesian parameter updating is efficient when a small number of interpretable power-law parameters dominate prognosis (Cheok et al., 2025). Physics-informed neural networks can be useful when sensor data are rich but the mapping from observation to crack state is nonlinear (Dourado & Viana, 2019; Liao et al., 2025). The present framework is deliberately algorithm-agnostic at the state-estimation layer so long as the posterior remains physically constrained and uncertainty is retained.

The NRC's digital-twin program is directly relevant to this work because it frames digital twins as synchronized systems that can provide diagnostics, visualizations, operations and maintenance recommendations, and potentially control signals (NRC, 2026). The same NRC program emphasizes technical challenges, regulatory considerations, advanced sensors, condition monitoring, and prognostic tools. For a crack-growth digital twin, this means model assurance cannot be postponed until after deployment. Measurement qualification, configuration control, uncertainty calibration, cybersecurity, data lineage, and human authorization should be architectural requirements.

ASME Section XI remains the governing technical reference for inservice inspection and flaw evaluation in light-water-cooled nuclear facilities. Its scope includes examination, NDE requirements, evaluation and acceptance standards, repair/replacement, and corrective actions (ASME, 2025). A practical digital twin should therefore produce outputs that can be consumed by Section XI engineering processes—for example, an updated flaw-size distribution or prioritized inspection recommendation—

without presenting its own probabilistic RUL as a code acceptance criterion unless and until such use is formally approved.

Figure 18: Assurance Architecture for a Nuclear Corrosion-Fatigue Digital Twin

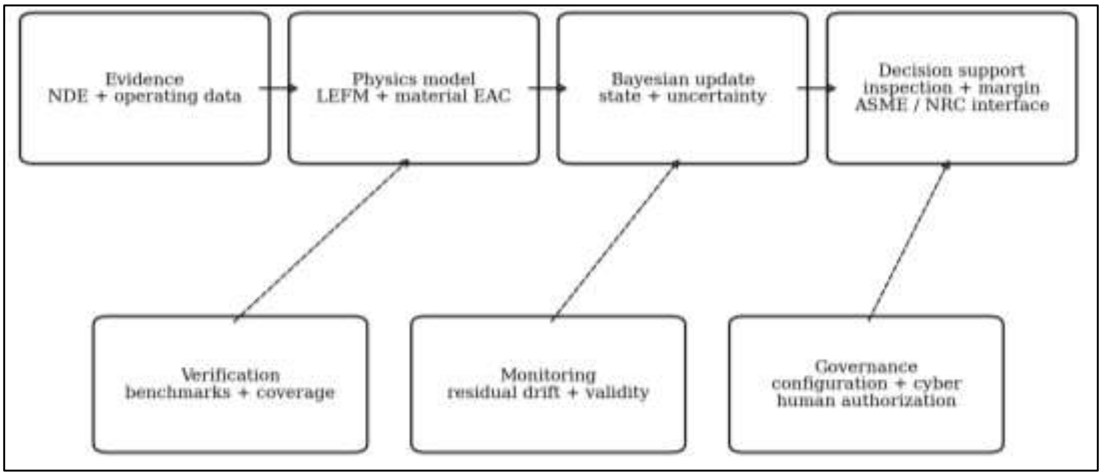

CONCLUSION

This study has developed a structured digital-twin methodology for corrosion-fatigue crack-growth prediction in 316L stainless steel and Alloy 690 for nuclear primary-circuit integrity assessment. The framework integrates fracture-mechanics crack-growth laws, material-specific environmental states, sequential Bayesian updating, uncertainty propagation, and risk-informed inspection support. The literature review demonstrates that this integration is physically justified: 316L environmental fatigue is strongly influenced by crack-growth acceleration and loading/environment interactions, while Alloy 690 exhibits high PWSCC resistance but retains state-dependent laboratory susceptibility associated with cold work, microstructure, local strain, and intergranular oxidation.

The physics-informed synthetic experiment demonstrates the analytical value of state synchronization. Static Paris-law predictions are improved by adding material/environment priors, and they are improved further when crack-size evidence updates the trajectory-specific growth state. The digital twin consequently tracks crack size more accurately, reduces RUL error, and produces uncertainty intervals that contract as evidence accumulates. These results do not establish new material properties; they establish that the proposed algorithmic architecture behaves coherently under controlled heterogeneity.

The principal engineering conclusion is that a corrosion-fatigue digital twin should be treated as a continuously updated integrity-information system rather than as an autonomous acceptance authority. Its most useful outputs are posterior flaw-state estimates, uncertainty bounds, future crack-growth distributions, probability-of-threshold-exceedance curves, and inspection-prioritization metrics. Code-required NDE, ASME Section XI flaw evaluation, licensing-basis requirements, and responsible engineering authorization remain the governing decision mechanisms. With qualified empirical calibration, such a twin could provide a defensible bridge between intermittent inspection evidence and continuous condition-informed nuclear aging management.

RECOMMENDATIONS

1. Build separate, traceable calibration datasets for 316L stainless steel and Alloy 690 rather than pooling them into a universal nuclear-alloy model. Dataset metadata should include heat/product form, orientation, heat treatment, cold work, weld/HAZ condition, temperature, dissolved hydrogen, boron/lithium chemistry, load ratio, waveform, frequency, crack size, and crack-measurement method.
2. Calibrate the crack-growth core against qualified ASTM E647-type fatigue-crack-growth data and environmentally assisted cracking datasets. For Alloy 690, include NRC-sponsored PWSCC datasets and distinguish solution-annealed, thermally treated, cold-worked, and welded conditions where data permit.

3. Replace the synthetic environmental multiplier used in this manuscript with material-specific empirical or mechanistic functions derived from independent training data. Preserve uncertainty around those functions so the model does not become falsely deterministic.
4. Couple component-specific finite-element or weight-function stress-intensity solutions to the digital twin. Residual stress, thermal transients, weld geometry, and crack-shape evolution should be represented at a fidelity commensurate with their influence on the integrity decision.
5. Use qualified NDE uncertainty models. Crack-size observations should enter the state estimator with probability-of-detection, sizing bias, repeatability, and coverage assumptions that reflect the actual inspection technology and examination conditions.
6. Evaluate multiple state-estimation algorithms—Bayesian parameter updating, extended/unscented Kalman filtering, particle filtering, and dynamic Bayesian networks—and select the simplest method that maintains calibrated uncertainty under the expected nonlinearities and data rates.
7. Perform chronological validation in which future operating periods are held out from model fitting. Random cross-validation can overstate performance for degradation processes because neighboring observations from the same crack trajectory are highly correlated.
8. Establish decision guardrails before deployment. The digital twin should be prevented from extending inspection or operating intervals beyond code- or program-defined maxima without explicit engineering review, regardless of a favorable posterior life estimate.
9. Implement model-drift monitoring. Residuals between predicted and observed crack states should be trended by material, component class, operating regime, and inspection method. Persistent bias should trigger revalidation or fallback to conservative baseline models.
10. Develop an auditable nuclear digital-twin assurance case that documents intended use, model validity domain, data provenance, software configuration, cybersecurity controls, uncertainty calibration, human authorization, failure modes, and conservative fallback behavior in alignment with ongoing NRC digital-twin research (NRC, 2025; NRC, 2026).

LIMITATIONS

The principal limitation is that the numerical dataset is synthetic. Although the model structure and qualitative sensitivities are supported by published literature, none of the synthetic Paris coefficients, environmental multipliers, crack trajectories, RUL errors, or risk curves should be used as material design data or plant-specific predictions.

The fracture-mechanics model is intentionally reduced-order. It does not include detailed threshold behavior, crack closure, full Forman/NASGRO transition behavior, cyclic plasticity, crack-shape evolution, mixed-mode loading, welding residual-stress redistribution, irradiation effects, oxide-film kinetics, or explicit stress-corrosion crack-growth terms. These mechanisms can be added in a component-specific implementation when supported by data.

The 316L and Alloy 690 environmental states are simplified. The dissolved-hydrogen response is not intended to reproduce a universal chemistry law, and the synthetic cold-work variable cannot represent all microstructural consequences of deformation. Alloy 690 PWSCC, in particular, depends on grain-boundary carbide state, fabrication history, orientation, and local microstructure in ways that a single scalar cold-work percentage cannot capture. The study assumes that crack size is observed directly with Gaussian error. Real nuclear NDE has detection thresholds, probability-of-detection behavior, sizing biases, access constraints, and examination-specific uncertainties. Future studies should model the full measurement process and should consider indirect sensors whose relationship to crack size requires its own validated diagnostic model.

The RUL threshold is a synthetic critical crack size rather than an ASME Section XI allowable flaw size. A real implementation must compute acceptance and fracture margins using component-specific stress analysis, material toughness, flaw geometry, and code requirements. The digital twin should not infer or redefine those regulatory thresholds. The simulation does not model future loading uncertainty in detail. Plant transients, flexible operation, thermal stratification, vibration, startup/shutdown frequency, and unanticipated events can change ΔK history materially. Operational digital twins should therefore assimilate actual transient histories and propagate scenario uncertainty rather than extrapolating a stationary load pattern. Finally, successful digital-twin deployment requires organizational as well as technical readiness. Data governance, cybersecurity, configuration management, model ownership, independent verification, and human decision authority can determine whether a technically accurate model is trustworthy in practice. These issues are especially important in safety-critical nuclear applications and are active subjects of NRC digital-twin research.

REFERENCES

[1]. Abdullah Mohammad, S. (2023). CUGAO₂ and CUINS₂ Quantum Dot Sensitization for Enhanced Photovoltaic Efficiency in Wearable Fiber-Shaped Solar Cells. American Journal of Advanced Technology and Engineering Solutions, 3(04), 209-261. https://doi.org/10.63125/wysdvy71

[2]. Alexandreanu, B., Chen, Y., & Natesan, K. (2023). Primary water stress corrosion cracking of high-chromium nickel-base welds—2018 (NUREG/CR-7276). U.S. Nuclear Regulatory Commission. https://www.nrc.gov/reading-rm/doc-collections/nuregs/contract/cr7276/index

[3]. American Society of Mechanical Engineers. (2025). BPVC Section XI, Division 1: Rules for inservice inspection of nuclear reactor facility components—Rules for inspection and testing of components of light-water-cooled plants. https://www.asme.org/codes-standards/find-codes-standards/bpvc-xi-bpvc-section-xi-rules-inservice-inspection-nuclear-power-plant-components

[4]. Ashrafuzzaman, M. (2024). The impact of cloud-based management information systems on hrm efficiency: an analysis of small and medium-sized enterprises (SMES). Academic Journal on Artificial Intelligence, Machine Learning, Data Science and Management Information Systems, 1(01), 40-56. https://doi.org/10.69593/ajaimldsmis.v1i01.124

[5]. ASTM International. (2024). ASTM E647-24: Standard test method for measurement of fatigue crack growth rates. https://doi.org/10.1520/E0647-24

[6]. Bruemmer, S. M., Toloczko, M. B., & Olszta, M. J. (2012). Pacific Northwest National Laboratory investigation of stress corrosion cracking in nickel-base alloys (NUREG/CR-7103, Vol. 2). U.S. Nuclear Regulatory Commission. https://www.nrc.gov/reading-rm/doc-collections/nuregs/contract/cr7103/v2/index

[7]. Cheok, E. W. W., Qian, X., Kaps, A., Quek, S. T., & Si, M. B. I. (2025). A strain-interfaced digital twin solution for corner fatigue crack growth using Bayesian inference. International Journal of Fatigue, 191, 108705. https://doi.org/10.1016/j.ijfatigue.2024.108705

[8]. Choi, K. J., Yoo, S. C., Jin, H.-H., Kwon, J., Choi, M.-J., Hwang, S. S., & Kim, J. H. (2016). Crack growth behavior of warm-rolled 316L austenitic stainless steel in high-temperature hydrogenated water. Journal of Nuclear Materials, 476, 243–254. https://doi.org/10.1016/j.jnucmat.2016.04.051

[9]. Chopra, O., & Stevens, G. L. (2018). Effect of LWR water environments on the fatigue life of reactor materials (NUREG/CR-6909, Revision 1). U.S. Nuclear Regulatory Commission. https://www.nrc.gov/reading-rm/doc-collections/nuregs/contract/cr6909/r1/index

[10]. Debasish, A. (2021). Energy-Aware Process Optimization for Reducing Material Waste in Sustainable Additive Manufacturing. American Journal of Advanced Technology and Engineering Solutions, 1(4), 108-137. https://doi.org/10.63125/j0wk7j48

[11]. Debasish, A. (2022). Simulation-Based Thermal Management Framework for Reducing Energy Consumption in Advanced Manufacturing Systems. International Journal of Scientific Interdisciplinary Research, 1(01), 335–381. https://doi.org/10.63125/6fcj7c89

[12]. Debasish, A. (2023). Thermal Behavior Modeling for Predicting Process Instability in Additive Manufacturing Systems. International Journal of Scientific Interdisciplinary Research, 4(4), 485-528. https://doi.org/10.63125/b2nemb48

[13]. Debasish, A. (2024). AI-Based Quality Control Framework for Reducing Rework and Scrap in Additive Manufacturing Production. Review of Applied Science and Technology, 3(04), 402–447. https://doi.org/10.63125/z29tv526

[14]. Debasish, A. (2025a). Design-for-Manufacturing Optimization for Improving Resilience in U.S. Additive Manufacturing Supply Chains. American Journal of Interdisciplinary Studies, 6(02), 185-204. https://doi.org/10.63125/hxm3tb71

[15]. Debasish, A. (2025b). Physics-Informed Machine Learning for Predicting Thermal Distortion in Metal Additive Manufacturing. American Journal of Scholarly Research and Innovation, 4(01), 943–989. https://doi.org/10.63125/ny974y17

[16]. Dourado, A., & Viana, F. A. C. (2019). Physics-informed neural networks for corrosion-fatigue prognosis. Annual Conference of the PHM Society, 11(1). https://doi.org/10.36001/phmconf.2019.v11i1.814

[17]. Edwards, C., López Morales, D., Haas, C., Narasimhan, S., & Cascante, G. (2023). Digital twin development through auto-linking to manage legacy assets in nuclear power plants. Automation in Construction, 148, 104774. https://doi.org/10.1016/j.autcon.2023.104774

[18]. Forman, R. G., Kearney, V. E., & Engle, R. M. (1967). Numerical analysis of crack propagation in cyclic-loaded structures. Journal of Basic Engineering, 89(3), 459–463. https://doi.org/10.1115/1.3609637

[19]. Fuller, A., Fan, Z., Day, C., & Barlow, C. (2020). Digital twin: Enabling technologies, challenges and open research. IEEE Access, 8, 108952–108971. https://doi.org/10.1109/ACCESS.2020.2998358

[20]. Hu, M., Zhang, X., Peng, C., Zhang, Y., & Yang, J. (2024). Current status of digital twin architecture and application in nuclear energy field. Annals of Nuclear Energy, 202, 110491. https://doi.org/10.1016/j.anucene.2024.110491

[21]. Huang, Q., Peng, S., & Deng, J. (2023). A review of the application of artificial intelligence to nuclear reactors: Where we are and what's next. Heliyon, 9(3), e13883. https://doi.org/10.1016/j.heliyon.2023.e13883

[22]. Jannatul, F. (2025). Spinal Cord Injury and Neurorehabilitation Deep Learning–Based Prediction of Functional Recovery Trajectories After Traumatic Spinal Cord Injury. ASRC Procedia: Global Perspectives in Science and Scholarship, 1(01), 2865–2922. https://doi.org/10.63125/m738bh82

[23]. Jones, D., Snider, C., Nassehi, A., Yon, J., & Hicks, B. (2020). Characterising the digital twin: A systematic literature review. CIRP Journal of Manufacturing Science and Technology, 29, 36–52. https://doi.org/10.1016/j.cirpj.2020.02.002

[24]. Kamaya, M. (2013). Environmental effect on fatigue strength of stainless steel in PWR primary water—Role of crack growth acceleration in fatigue life reduction. International Journal of Fatigue, 55, 102–111. https://doi.org/10.1016/j.ijfatigue.2013.05.008

[25]. Kamaya, M. (2017). Influence of strain range on fatigue life reduction of stainless steel in PWR primary water. Fatigue & Fracture of Engineering Materials & Structures, 40(12), 2194–2203. https://doi.org/10.1111/ffe.12650

[26]. Kamaya, M. (2020). Environmental effect of PWR primary water on fatigue life of stainless steel (influence of loading rate on fatigue life reduction). Fatigue & Fracture of Engineering Materials & Structures, 43, 2571–2581. https://doi.org/10.1111/ffe.13277

[27]. Kim, W., Lee, G., Son, H., Choi, H., & Youn, B. D. (2022). Estimation of fatigue crack initiation and growth in engineering product development using a digital twin approach. Reliability Engineering & System Safety, 229, 108721. https://doi.org/10.1016/j.ress.2022.108721

[28]. Kuang, W., & Was, G. S. (2020). A high-resolution characterization of the initiation of stress corrosion crack in Alloy 690 in simulated pressurized water reactor primary water. Corrosion Science, 163, 108243. https://doi.org/10.1016/j.corsci.2019.108243

[29]. Kuang, W., Song, M., & Was, G. S. (2018). Insights into the stress corrosion cracking of solution annealed Alloy 690 in simulated pressurized water reactor primary water under dynamic straining. Acta Materialia, 151, 321–333. https://doi.org/10.1016/j.actamat.2018.04.002

[30]. Kuang, W., Yue, H., Feng, X., Yang, B., & Guo, C. (2020). A novel test technique for the mechanistic study of initiation of environmentally assisted cracking on a Ni–30Cr–10Fe alloy in simulated pressurized water reactor primary water. Scripta Materialia, 189, 122–128. https://doi.org/10.1016/j.scriptamat.2020.08.016

[31]. Liao, W., Long, X., & Jiang, C. (2025). A physics-informed neural network method for identifying parameters and predicting remaining life of fatigue crack growth. International Journal of Fatigue, 191, 108678. https://doi.org/10.1016/j.ijfatigue.2024.108678

[32]. Lou, X., Othon, M. A., & Rebak, R. B. (2017). Corrosion fatigue crack growth of laser additively-manufactured 316L stainless steel in high temperature water. Corrosion Science, 127, 120–130. https://doi.org/10.1016/j.corsci.2017.08.023

[33]. Md Anisur Rahman, M. (2024). State Income Tax Differentials and High-Skilled Labor Mobility in The United States: A Time Series Analysis. American Journal of Interdisciplinary Studies, 5(04), 222-267. https://doi.org/10.63125/295bsn47

[34]. Md Anisur Rahman, M. (2025). The Role of AI-Enabled Business Intelligence in Financial Risk Assessment and Liquidity Monitoring. Review of Applied Science and Technology, 4(04), 195–246. https://doi.org/10.63125/p4eezd93

[35]. Md Arif Uz, Z., Sharmin, S., & Md Abdur, R. (2025). Factors Influencing Behavioural Intention to Use he Innovative Open And Distance Learning Systems With The Role Of Continuance Intention. American Journal of Scholarly Research and Innovation, 4(01), 202-220. https://doi.org/10.63125/pbjxp014

[36]. Md Ashfaq, S., & Abdullah Mohammad, S. (2022). CNT/PANI Composite Electrodes for Flexible Fiber-Shaped Dye-Sensitized Solar Cells: Synthesis, Characterization, and Photovoltaic Performance. American Journal of Interdisciplinary Studies, 3(02), 221-274. https://doi.org/10.63125/m334mf41

[37]. Md Asif Ali Sheak, A., & Risha, A. (2022). The Role of IOT-Driven Energy Analytics in Improving Operational Efficiency and Sustainability in Modern Industrial Facilities. American Journal of Interdisciplinary Studies, 3(04), 807-841. https://doi.org/10.63125/gm63q956

[38]. Md Kaium, H. (2023). A GIS-Based Multi-Criteria Decision-Support and Land-Suitability Optimization Framework for Climate-Resilient Urban and Regional Planning. American Journal of Data Science and Analytics, 4(06), 43–103. https://doi.org/10.63125/wvq0sx87

[39]. Md Kaium, H. (2024). Machine Learning Enhanced GIS And AHP Modeling for High-Resolution Flood-Susceptibility Prediction, Vulnerability Assessment, and Risk Classification. Review of Applied Science and Technology, 3(02), 92–140. https://doi.org/10.63125/fz8hv245

[40]. Md Kaium, H. (2025). Integrating Artificial Intelligence, Semantic Indoor Geospatial Modeling, And Network-Based Routing for High-Precision NG911 Emergency Location Intelligence. International Journal of Scientific Interdisciplinary Research, 6(1), 616–670. https://doi.org/10.63125/5hc1xx56

[41]. Md Mahamud Pervaz, P. (2023). Integration of MES, SAP, And PI Historian Platforms for Real-Time Industrial Asset Performance Management. Review of Applied Science and Technology, 2(04), 393–445. https://doi.org/10.63125/9ebtas97

[42]. Md Mahamud Pervaz, P. (2025). Development of a CMMS-Integrated Predictive Maintenance Framework for Industrial PLC and Drive Systems. American Journal of Scholarly Research and Innovation, 4(01), 894–942. https://doi.org/10.63125/j33gtf31

[43]. Md. Abdur, R., & Iftekhar, A. (2021). Customer Retention Forecasting in Mobile Wallet Services Using Neural Networks: A Comparative Quantitative Study. International Journal of Business and Economics Insights, 1(4), 70-102. https://doi.org/10.63125/dyrpc387

[44]. Md. Rashedul, I., & Md Kaium, H. (2022). Development Of a Three-Dimensional Indoor Geospatial Network and Address Geocoding Framework for Next-Generation Emergency Dispatch and Response-Time Optimization. Journal of Sustainable Development and Policy, 1(02), 245-292. https://doi.org/10.63125/tcw3mp48

[45]. Md. Shakhawat, H., & Md, F. (2024). Impact of Phishing Simulation Campaigns and Security Awareness Training on Human Risk Mitigation in Financial Institutions: A Quantitative Study. American Journal of Data Science and Analytics, 5(10), 48-85. https://doi.org/10.63125/4j8h1484

[46]. Mohammad Abir Chowdhury, S. (2023). Role of AI-Assisted Risk Assessment in Enhancing Audit Planning Efficiency and Risk Prioritization in Public-Safety Organizations. International Journal of Scientific Interdisciplinary Research, 4(4), 529–576. https://doi.org/10.63125/qd6nn437

[47]. Mohammad Abir Chowdhury, S. (2025). Application of Machine Learning and Anomaly-Detection Algorithms for Fraud Detection in U.S. Government Financial Operations. American Journal of Interdisciplinary Studies, 6(02), 139-184. https://doi.org/10.63125/fkf19309

[48]. Mohammad Abir Chowdhury, S., & Tonay, P. (2022). An Empirical Analysis of the Impact of Robotic Process Automation and Continuous Auditing on the Timeliness And Accuracy Of Financial Reporting Assurance. International Journal of Business and Economics Insights, 2(4), 73-126. https://doi.org/10.63125/7p8dcr47

[49]. Mohammad Badrul, A. (2025). SCADA And IOT-Enabled Smart Water Metering: A Systematic Review of Resilient Supply Monitoring. International Journal of Scientific Interdisciplinary Research, 6(1), 576–615. https://doi.org/10.63125/at8pnx81

[50]. Mohammad Shoriful Hossan, S. (2022). A Performance-Based Framework for Arc-Flash Hazard Reduction and Electrical Reliability Improvement in Brownfield Industrial Distribution Systems. Review of Applied Science and Technology, 1(04), 447-463. https://doi.org/10.63125/a70vj720

[51]. Mst Kaniz, F. (2022). Language Access and Health Equity: Role of Multilingual Administrative Staff in Reducing Healthcare Disparities Among South Asian Immigrant Communities in The U.S. International Journal of Scientific Interdisciplinary Research, 1(01), 274–315. https://doi.org/10.63125/xqhss825

[52]. Mukahiwa, K., Scenini, F., Burke, M. G., Platts, N., Tice, D. R., & Stairmand, J. W. (2018). Corrosion fatigue and microstructural characterisation of Type 316 austenitic stainless steels tested in PWR primary water. Corrosion Science, 131, 57–70. https://doi.org/10.1016/j.corsci.2017.10.022

[53]. Nishat, J. (2023). Communicable Disease Prevention in a Post-Pandemic Era: A Global Review of Public Health Education, Surveillance, and Community-Level Interventions. International Journal of Scientific Interdisciplinary Research, 4(4), 630–678. https://doi.org/10.63125/mnqefj36

[54]. Nishat, J. (2025). Leveraging Machine Learning to Identify and Address Maternal Health Disparities in Underserved U.S. Communities. American Journal of Data Science and Analytics, 6(12), 125-169. https://doi.org/10.63125/c2t7r719

[55]. Nishat, J., & Jahanara, A. (2024). Machine Learning Approaches for Early Prediction of High-Risk Pregnancy in Underserved U.S. Populations. American Journal of Interdisciplinary Studies, 5(04), 268-309. https://doi.org/10.63125/5gh5df13

[56]. Nishat, J., & Mst Kaniz, F. (2022). A Review of the Impact of Covid-19 On Maternal and Child Health Service Utilization in Bangladesh. American Journal of Scholarly Research and Innovation, 1(02), 223–269. https://doi.org/10.63125/vgv5s742

[57]. Nuzhat Sadia, P. (2025). Integrating Business Intelligence Dashboards for Real-Time Supply Chain Visibility and Operational Decision Support. American Journal of Data Science and Analytics, 6(12), 170-216. https://doi.org/10.63125/1es4f763

[58]. Paris, P., & Erdogan, F. (1963). A critical analysis of crack propagation laws. Journal of Basic Engineering, 85(4), 528–533. https://doi.org/10.1115/1.3656900

[59]. Sadia, Z. (2025). Predictive Analytics for Financial Performance Forecasting and Reporting Quality: Evidence from Data-Driven Financial Management Systems. ASRC Procedia: Global Perspectives in Science and Scholarship, 1(01), 2795–2812. https://doi.org/10.63125/zstqn346

[60]. Shaiful, M., Anisur, R., & Md, A. (2022). A Systematic Literature Review on the Role of Digital Health Twins in Preventive Healthcare For Personal and Corporate Wellbeing. American Journal of Interdisciplinary Studies, 3(04), 1-31. https://doi.org/10.63125/negjw373

[61]. Toloczko, M. B., Overman, N. R., Olszta, M. J., & Bruemmer, S. M. (2016). Pacific Northwest National Laboratory investigation of stress corrosion cracking in nickel-base alloys: Stress corrosion cracking of cold worked Alloy 690 (NUREG/CR-7103, Vol. 3). U.S. Nuclear Regulatory Commission. https://www.nrc.gov/reading-rm/doc-collections/nuregs/contract/cr7103/v3/index

[62]. Tonay, P. (2025). Machine Learning for Fraud Detection in Enterprise Financial Systems. American Journal of Advanced Technology and Engineering Solutions, 1(02), 304-318. https://doi.org/10.63125/d0fhp873

[63]. Tonay, P., Md Maruf, I., & Al, A. (2024). Artificial Intelligence-Based Decision Support Systems and Managerial Performance. American Journal of Advanced Technology and Engineering Solutions, 4(04), 154-184. https://doi.org/10.63125/wmz8dc67

[64]. U.S. Nuclear Regulatory Commission. (2018). Regulatory Guide 1.207, Revision 1: Guidelines for evaluating fatigue analyses incorporating the life reduction of metal components due to the effects of the light-water reactor environment for new reactors. https://www.nrc.gov/reading-rm/doc-collections/reg-guides/power-reactors/rg/division-1/division-1-201

[65]. U.S. Nuclear Regulatory Commission. (2025). Technical assessment of the application of digital twin and prognostic tools for condition monitoring (RES-DE-REB-2025-09). https://www.nrc.gov/reading-rm/doc-collections/technical-letter-reports/2025/index

[66]. U.S. Nuclear Regulatory Commission. (2026). Digital twins. https://www.nrc.gov/reactors/power/digital-twins

[67]. Uddin, H. M. M., & Risha, A. (2024). Hybrid Cloud Security and Compliance in U.S. Enterprises: Addressing Data Privacy Risks and Governance Challenges. American Journal of Scholarly Research and Innovation, 3(01), 153–197. https://doi.org/10.63125/qcy0cj46

[68]. Walker, K. (1970). The effect of stress ratio during crack propagation and fatigue for 2024-T3 and 7075-T6 aluminum. In Effects of environment and complex load history on fatigue life (ASTM STP 462, pp. 1–14). ASTM International. https://doi.org/10.1520/STP32032S

[69]. Wang, M., Feng, S., Incecik, A., Królczyk, G., & Li, Z. (2022). Structural fatigue life prediction considering model uncertainties through a novel digital twin-driven approach. Computer Methods in Applied Mechanics and Engineering, 391, 114512. https://doi.org/10.1016/j.cma.2021.114512

[70]. Yonezawa, T., Watanabe, M., & Hashimoto, A. (2015). The effects of metallurgical factors on PWSCC crack growth rates in TT Alloy 690 in simulated PWR primary water. Metallurgical and Materials Transactions A, 46, 2768–2780. https://doi.org/10.1007/s11661-015-2852-1

[71]. Zhai, Z., Toloczko, M. B., Kruska, K., & Bruemmer, S. M. (2017). Precursor evolution and stress corrosion cracking initiation of cold-worked Alloy 690 in simulated pressurized water reactor primary water. CORROSION, 73(10), 1224–1236. https://doi.org/10.5006/2470

[72]. Zhang, W., Chen, Y., He, X., Xue, F., Xu, P., & He, W. (2026). Real-time fatigue crack growth prediction for welded structures based on digital twin framework considering residual stress and variable amplitude loading. International Journal of Fatigue, 206, 109475. https://doi.org/10.1016/j.ijfatigue.2025.109475